Journal of Mammalian Evolution (2025) 32:40
https://doi.org/10.1007/s10914-025-09785-0

RESEARCH

The brain endocast of the Canary Islands giant rats (*Canariomys*, Muridae, Rodentia): paleobiological and evolutionary implications

Flavien Vincent[1,2] · Antoine Souron[1] · Isaac Casanovas-Vilar[2] · Jesús Gamarra[2] · Ornella C. Bertrand[2,3]

Received: 16 July 2025 / Accepted: 26 October 2025

Abstract

Insular mammal faunas have been the focus of numerous studies in evolutionary biology, specifically regarding the patterns of dwarfism and gigantism. Previous work has shown either increase or decrease in relative brain size in various clades, including elephants, hippos, lagomorphs, bovids, and multituberculates. Decrease in specific senses such as audition and vision were also observed. In this study, we describe the virtual brain endocasts of the giant rats of the Canary Islands, *Canariomys bravoi* and *Canariomys tamarani*, and make morphological and quantitative comparisons with 10 extant mainland and insular Murinae. We measured endocranial volumes and the relative sizes of brain regions, including the olfactory bulb and petrosal lobule volumes and the neocortical and paleocortex surface areas. Our results show that intraspecific variation was higher in *Ca. bravoi* compared to its closest extant relative *Arvicanthis niloticus*, which supports the idea that phenotypic variability is more prevalent on islands than on the continent. *Canariomys tamarani* could represent an intermediate form between *Arvicanthis* and *Ca. bravoi*, as previously hypothesized. The midbrain exposure in *Ca. bravoi* is likely a derived feature due to the reduction in the neocortex. The relatively small size of the olfactory bulbs in *Canariomys* might be related to decreased predation risk. The relatively smaller petrosal lobules in *Ca. tamarani* and insular extant rodents could have resulted from a shift to slower locomotion compared to their mainland relatives. Overall, we show that, as in the insular lagomorph *Nuralagus rex*, decrease in various senses has also occurred in rodents living on islands.

Keywords Brain endocast · Canary islands · Gigantism · Insular mammals · Island effect · Pleistocene

Introduction

Islands are complex ecosystems, and specific biological rules have been described for animals and plants living on them. One of the most spectacular patterns is small-animal gigantism and large-animal dwarfism in relation to mainland relatives (Van Valen 1973; Lomolino et al. 2012, 2013; Benítez-López et al. 2021). However, insular animals also show many adaptive traits, including dental adaptations (i.e., increase in hypsodonty with the addition of lophs, larger cheek teeth), a shortening of the distal part of the hindlimb and a low gear locomotion (Sondaar 1977; Van Der Geer et al. 2021). However, none of these adaptations are consistently present across insular taxa (Van Der Geer 2014). The insular models have been tested for mammals (e.g., Lomolino 1985; Bromham and Cardillo 2007; Meiri et al. 2008; McFadden et al. 2013; Benítez-López et al. 2021), amphibians (Montesinos et al. 2012; Benítez-López et al. 2021), birds (Clegg and Owens 2002; Boyer and Jetz 2010; Benítez-López et al. 2021), reptiles (Boback 2003; Itescu et al. 2014; Benítez-López et al. 2021), fish (Herczeg et al. 2009), insects (Palmer 2002), and plants (Biddick et al. 2019). Some of these studies only focused on a small number, which might not represent an entire clade. Recently, Benítez-López et al. (2021) showed

✉ Flavien Vincent
flavienvincent85@gmail.com

✉ Ornella C. Bertrand
ornella.bertrand@icp.cat

[1] Université de Bordeaux, CNRS, Ministère de la Culture, PACEA, UMR 5199, Pessac F-33600, France

[2] Institut Català de Paleontologia Miquel Crusafont (ICP-CERCA), Universitat Autònoma de Barcelona, Edifici ICTA-ICP, c/ Columnes s/n, Campus de la UAB, Cerdanyola del Vallès (Barcelona) 08193, Spain

[3] Section of Mammals, Carnegie Museum of Natural History, Pittsburgh, PA, USA

Published online: 25 December 2025

that a significant change in body mass occurs between mainland and island species, and corroborated the island rule for mammals, birds, and reptiles but not for amphibians. Some factors responsible for this change in body mass have been identified and include island size, spatial isolation, temperature, and seasonality. Various hypotheses have been proposed as selective pressures underlying the insular forms, including low predation pressure, low interspecific competition, and resource limitation (Lomolino 1985, 2005; Benítez-López et al. 2021). Many examples of insular forms are known from the fossil record, including proboscideans, cervids, bovids, hippopotamids, hominins, multituberculates, and dinosaurs (e.g., Bate 1909; Brown et al. 2004; Benton et al. 2010; Csiki-Sava et al. 2018).

Many studies have described and quantified changes in shape and size of the brain of mammals throughout geological times using virtual (or natural) brain endocasts of extinct and extant species, including but not limited to early mammals (e.g., Macrini et al. 2007; Rowe et al. 2011), proboscideans (Benoit et al. 2013), artiodactyls (Orliac and Gilissen 2012; Orliac et al. 2023), carnivorans (Flink and Werdelin 2022), rodents (e.g., Bertrand and Silcox 2016; Bertrand et al. 2018), and primates (e.g., Silcox et al. 2010; Harrington et al. 2016). However, few studies have explored the impact of living on islands on the brain of vertebrates. Lyras (2018) found that insular elephants and hippos were not only small versions of the mainland species, but they also showed an increase in relative brain size. Quintana et al. (2011) also found that *Nuralagus rex*, a giant lagomorph from Minorca (Balearic Islands, Spain), had relatively small-sized sense-related regions of the cranium (i.e., tympanic bullae, orbits, choanae, and braincase) compared to its mainland relatives (*Oryctolagus*). They interpreted this result as a reduction of its sensory organs and a reduced brain size. Similar results were found for the endemic bovid *Myotragus* from Majorca (Spain) and the Cretan deer *Candiacervus*. They both show a brain size reduction of 45% to 50% for *Myotragus* and 13% to 22% for *Candiacervus* (Köhler and Moyà-Solà 2004; Palombo et al. 2008). However, Liakopoulou et al. (2024) found that the brain size reduction of *Myotragus* may have only been 17% smaller compared to contemporaneous Late Miocene taxa. More recently, Orgebin et al. (2025) published the virtual endocast of a Late Miocene ruminant from Gargano (Italy), *Hoplitomeryx matthei*. A minor brain size reduction and no reduction in the occipital region of the neocortex or in the olfactory bulbs were found. Because great uncertainty remains regarding its closest continental relative, these results might have to be reassessed in the future. In contrast, the question of insular gigantism and its impact on the brain has been underexplored in mammals, with the only studies being those by Blanco-Lapaz (2005, 2007) on the rodent *Canariomys* from the Canary Islands in Spain and on the lagomorph *Nuralagus* from Minorca (Quintana et al. 2011). In his results, Blanco-Lapaz (2005, 2007) did not find any differences in relative brain size between *Canariomys* and other mainland rodents. However, based on the previous research of Quintana et al. (2011), we may expect a decrease in senses in *Canariomys*.

The Canary Islands are a chain of seven main islands (Fig. 1). At 100 km west of Morocco, these islands are not larger than 7,500 km^2 and are among the most studied islands in the world in terms of geology, vegetation structure, and climate (Walter 1979; Fernández-Palacios et al. 2011; Suchodoletz et al. 2012). The Canary Islands have a diverse set of climatic conditions. The eastern islands (Fuerteventura and Lanzarote) have a Mediterranean climate, which results in subdesertic habitats with scrublands and relatively low elevations (less than 800 m). The lowlands of Gran Canaria and Tenerife have a similar climate, but in high elevations (from 500 to 1200 m) more precipitation and less seasonality occur, which would be similar to Oligocene and Miocene Eurasian forests (Del Arco Aguilar et al. 2018). Two extinct giant rodents are found in this archipelago, *Canariomys bravoi* in Tenerife and *Canariomys tamarani* in Gran Canaria. *Canariomys bravoi* was discovered in the 1950 s by Telesforo Bravo and described by Crusafont-Pairó and Petter (1964), who erected the species and the genus based on a cranium found in the Late Pleistocene site of la Cueva de las Palomas (translated as 'Cave of the Doves') in Tenerife. Crusafont-Pairó and Petter (1964) did not formally designate a holotype. Although Martínez Méndez (1966) stated that a cranium was the holotype, this work was never published. More recently, the type cranium of *Ca. bravoi* was identified in the Institut Català de Paleontologia Miquel Crusafont (ICP) collections and described in detail comparing both cranial and dental morphology to that of extant murines (Casanovas-Vilar and Luján 2022).

Partial nuclear and mitochondrial DNA data estimate the divergence time between *Ca. bravoi* and *Arvicanthis* grp *niloticus* (extant populations from Masai Mara) at around 650,000 years ago. The oldest and youngest fossils of *Ca. bravoi* are respectively dated to 17,300 cal BP (calibrated years before present) and 2,265 ± 85 cal BP (Crowley et al. 2019). Recently, ancient DNA from *Ca. bravoi* showed that this species is nested within the genus *Arvicanthis* (African grass rats), revealing that the genus *Arvicanthis* is paraphyletic (Renom et al. 2021). *Arvicanthis* is a well-known genus represented exclusively by African species, ranging from Egypt to Tanzania and from Senegal to Somalia (Lesson 1842; Fadda and Corti 2001). This genus lives in a wide range of habitats, including arid regions, steppes, shrublands, wooded savannahs, forest-savannah mosaic, and wetlands (Lecompte et al. 2008; Dobigny et al. 2013; Aghová et al. 2018).

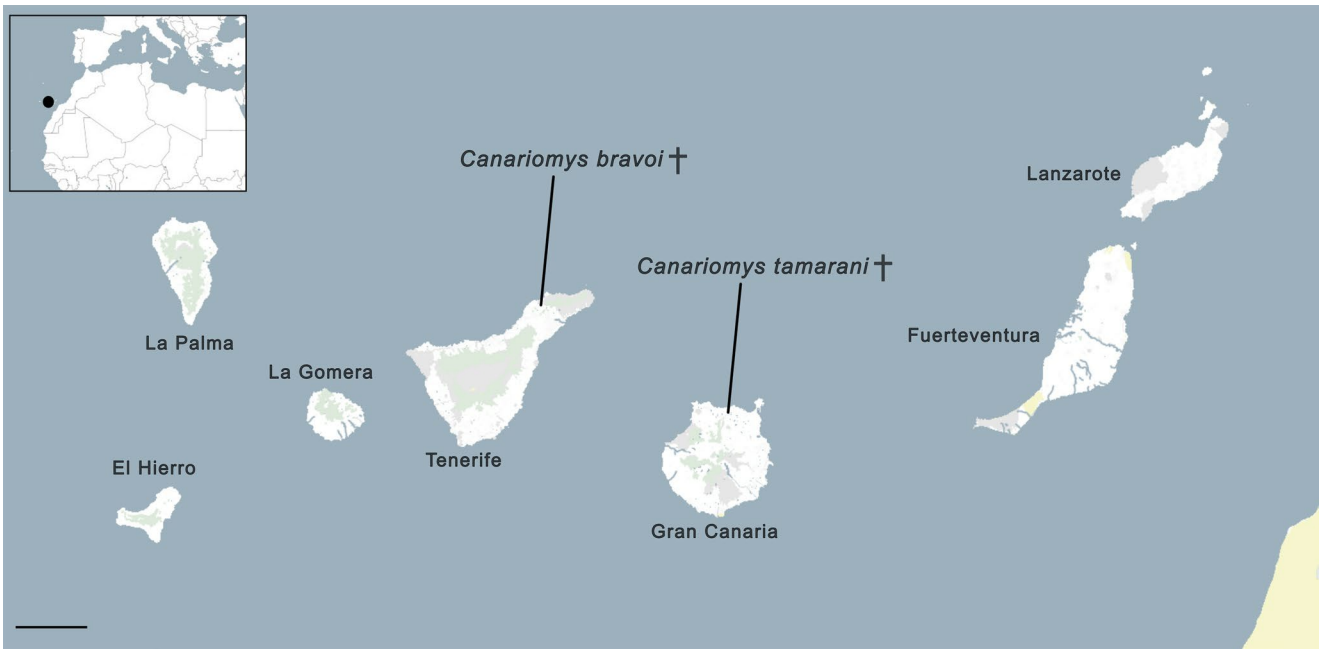

Fig. 1 Geographic map of the Canary Islands and localisation of both *Canariomys* species. Map designed using Mapcreator

Based on stomach content, the various *Arvicanthis* species have an omnivorous diet that changes seasonally, with a high consumption of plants in the dry season, whereas animal matter is consumed during the rainy season (Rabiu and Fisher 1989). Using faecal analyses, *Arvicanthis* was also recovered as omnivore (Delany and Monro 1986). However, two studies concluded that *Arvicanthis* was more herbivorous based on stomach content and isotopic values (Taylor and Green 1976; Bergstrom 2013). Based on cranial and dental measurements, the body mass of *Ca. bravoi* has been estimated to ~1.5 kg (Moncunill-Solé et al. 2014), which is 14 times heavier than the mean body mass of *A. niloticus* (Renom et al. 2021).

Based on postcranial data, Michaux et al. (2012) proposed that *Ca. bravoi* was a predominantly ground-dwelling animal with a heavily built skeleton but also showed some digging and scansorial/arboreal adaptations. *Canariomys bravoi* was found to have an herbivorous diet with a predominance of C_3 plants based dental microwear, mandible geometric morphometrics, and carbon ($\delta^{13}C$) and nitrogen ($\delta^{15}N$) stable isotopes from bone collagen (Bocherens et al. 2003, 2006; Firmat et al. 2010). However, a more recent study found slightly more positive $\delta^{13}C$ and $\delta^{15}N$ values, which would be indicative of a more omnivorous diet (Crowley et al. 2019).

López-Jurado and López Martínez (1987) erected a second species, *Canariomys tamarani*, from the Gran Canaria Island, and further described the dental anatomy of the genus, proposing a differential diagnosis for *Ca. bravoi* and *Ca. tamarani*. *Canariomys tamarani* was interpreted as a rodent with an herbivorous diet and a ground-dwelling lifestyle, including some digging abilities. This taxon had a body mass of approximately 1 kg, which is close to the body mass of *Ca. bravoi* (Moncunill-Solé et al. 2014). *Canariomys tamarani* has been placed within the Arvicanthini tribe based on the analysis of its dental and skull morphology (López-Jurado and López Martínez 1987; Hutterer et al. 1988; Casanovas-Vilar and Luján 2022). However, its cranial anatomy is more similar to *Ca. bravoi* than *Arvicanthis* (Casanovas-Vilar and Luján 2022). Interestingly, the dental morphology of *Ca. tamarani* is not as derived as in *Ca. bravoi*, being more reminiscent of that of *A. niloticus* (Casanovas-Vilar and Luján 2022). These findings are important as *Ca. tamarani* was discovered in Gran Canaria, which is closer to the African continent (Fig. 1). Recent studies concluded that both *Canariomys* species would have derived from small populations of *A. niloticus*, which would have reached the Canary Islands via passive rafting from the African mainland (Renom et al. 2021; Casanovas-Vilar and Luján 2022).

In this paper, we describe the brain endocast of two specimens of *Ca. bravoi* and one specimen of *Ca. tamarani*. We compare their endocasts with those of 10 extant species of Muridae. The aim of this study is to answer the following questions: (1) how did the brain endocast of *Canariomys* evolve in the context of insularity?; (2) can the study of the brain endocast of *Ca. bravoi* inform about the ecology of this species?; and (3) are there any common neurobiological and sensory patterns found in insular mammals?

Materials and methods

Comparative sample Our sample is composed of 13 specimens belonging to 11 different species (Fig. 2; Table 1). The scanning parameters are detailed in Online Resource 1: Table S1. The fossil sample is composed of two specimens of *Ca. bravoi* and one specimen of *Ca. tamarani*. We also included three species of *Arvicanthis* (i.e., *Arvicanthis niloticus*, *Arvicanthis neumanni*, and *Arvicanthis abyssinicus*) and chose to include two specimens of *A. niloticus* from different localities, one from Mali and another one from Central African Republic. The specimen MNHN-ZM-MO-1978-195 of *A. neumanni* is from the Muséum national d'Histoire naturelle (MNHN) collections and was studied by Michaux et al. (2012) but referred to *A. niloticus* with number "n195". The only *Arvicanthis* specimen in the MNHN collection with this number is the specimen MNHN-ZM-MO-1978-195, currently assigned to *A. neumanni*.

The rest of the sample is composed of six other extant species of murine rodents: three closely-related species of

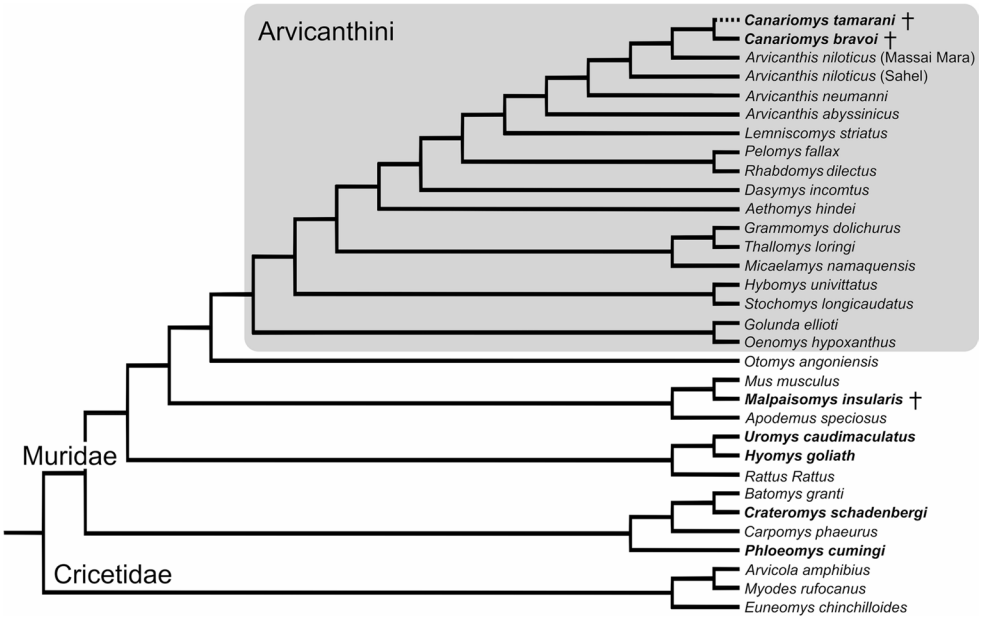

Fig. 2 Simplified phylogenetic tree showing the position of two species of *Canariomys* within Muridae based on Casanovas-Vilar and Luján (2022; data from Steppan and Schenk 2017; Aghová et al. 2018; Bryja et al. 2019; and Renom et al. 2021). Insular species are in bold, and extinct species are indicated with †

Table 1 Information on the specimens included in this study

Species	Collection number	Collection	Locality	Reference	Age	Island species
Canariomys bravoi	IPS36548	ICP	La Cueva de las Palomas Tenerife	Casanovas-Vilar and Luján (2022)	Late Pleistocene	Yes
Canariomys bravoi	TFMCVF873	MUNA	Cueva del Viento, Tenerife	Michaux et al. (2012)	Holocene	Yes
Canariomys tamarani	ZFMK 2010.308	ZFAK	Unknown	Michaux et al. (2012)	Unknown	Yes
Arvicanthis niloticus	MNHN-ZM-MO-1998-1113	MNHN	Central African Republic	-	Extant	No
Arvicanthis niloticus	MNHN-ZM-MO-2004-750	MNHN	Mali	-	Extant	No
Arvicanthis neumanni	MNHN-ZM-MO-1978-195	MNHN	Ethiopia	Michaux et al. (2012)	Extant	No
Arvicanthis abyssinicus	MNHN-ZM-MO-1905–213 A	MNHN	Kisumu, Kenya	-	Extant	No
Lemniscomys striatus	MNHN-ZM-2008-6	MNHN	Guinea	-	Extant	No
Pelomys fallax	MNHN-ZM-MO-2007-1247	MNHN	Selous, Ngarembe village, Tanzania	-	Extant	No
Rhabdomys dilectus	MNHN-ZM-2005-688	MNHN	Olkokola, Tanzania	-	Extant	No
Rattus rattus	M-443	PACEA	Guadeloupe	Goedert et al. (2020)	Extant	No
Craterомys schadenbergi	MNHN-ZM-MO-1897-414	MNHN	Luzon, Philippines	-	Extant	Yes
Phloeomys cumingi	MNHN-ZM-AC-A7569	MNHN	Manila, Philippines	-	Extant	Yes

Arvicanthini (*Lemniscomys striatus*, *Pelomys fallax*, *Rhabdomys dilectus*), two large-sized insular species of Phloeomyini (*Crateromys schadenbergi* and *Phloeomys cumingi*), and one species of Rattini (*Rattus rattus*). The specimen PACEA-M-443 of *Ra. rattus* is from Guadeloupe (France) and was captured for a study of the seasonal demography of black rat populations (Goedert et al. 2020). Even if this specimen is from an island, it is a very recent introduction. The brain endocast of *Ra. rattus* from Guadeloupe has been the focus of another study by Vincent et al. (2023). These island rats have not been compared to mainland populations. It is possible that they may show differences (see Van Der Geer et al. 2018), but the intraspecific variation would likely be smaller than interspecific variation and therefore, the inclusion of an island rat should not affect the results of the present study. Locality, age, and island status for the sample are detailed in Table 1.

Canariomys bravoi IPS36548 is a nearly complete cranium that is only lacking the bullae and a part of the left zygomatic arch. This specimen was found in La Cueva de las Palomas site, Acantilado de Martiánez (Puerto de la Cruz, Tenerife, Canary Islands), estimated to be Late Pleistocene in age (129,000–11,700 years; boundaries after Gibbard and Head 2020). A second specimen of *Ca. bravoi* (TFMCVF873) is a nearly complete cranium that is also lacking the auditory region. This specimen is from el Museo de la Naturaleza y el Hombre, Santa Cruz (Tenerife, Canary Islands). The specimen was found in 1982 by J.-J. Hernández Pacheco in the Cueva del Viento site (Icod de los Vinos, Tenerife). Bones from the same site assigned to *Ca. bravoi* have been ^{14}C dated to 12,230 ± 140 cal BP (Michaux et al. 1996). This age has been recalibrated by Crowley et al. (2019) to 14,290 ± 535 Cal BP. The specimen ZFMK 2010.308 has been identified as *Ca. tamarani* (see differential diagnosis from López-Jurado and López Martínez 1987). It was collected in 1984 by R. Hutterer and L.F. López-Jurado in the Ingenio lava tube, but the exact location and the site are unknown. The cranium is complete and undistorted. The geological age, locality, and other information about the specimen are unknown.

We provide detailed anatomical comparisons of *Canariomys* with its closest extant relative *Arvicanthis* (*A. niloticus*, *A. neumanni*, and *A. abyssinicus;* Fig. 3a-g). For the principal component analysis (PCA), we include the remaining of the sample (Fig. 3h-m) to study the variation in brain size and its components in a broader context of insular vs. mainland species of murines.

Virtual endocast acquisition

The virtual endocasts of all specimens were semi-automatically segmented using the 3D data processing software Avizo 2019.1 (Visualization and Sciences Group 1995—2019). For each specimen, we segmented one slice approximately every 30 slices and every 10 slices for regions with more anatomical variations along the endocast, including the olfactory bulbs. When the bone was missing, a straight line was traced from the two nearest pieces of preserved bone. Then, we used the software Biomedisa v23.09.1–226.1-g1a807f7 (Lösel et al. 2020) to automatically segment the rest of the slices. Biomedisa uses bone density from the CT scans and the segmented slices (i.e., labelfield module) to interpolate the remaining endocranial cavity (Lösel et al. 2020). Subsequently, the labelfield module containing the virtual endocasts was re-opened in Avizo and manually cleaned to eliminate any errors introduced by Biomedisa. Two labelfield modules were created to obtain an image showing the endocast inside a translucent cranium (Fig. 3). Additionally, two different materials were created to differentiate the brain endocast from vessel and nerve casts in order to not overestimate the endocranial size. A new labelfield module was created based on the slices containing the brain endocast only, and a surface rendering of the brain endocast was obtained.

Brain endocranial quantifications

The volume of the virtual brain endocast was obtained with the function "surface area volume" in Avizo. The olfactory bulbs were isolated using the "volume edit" function and then the "generate surface" function was used to create a new surface. The volume of this new surface was generated with the same function as for the brain endocast to calculate the volume of the olfactory bulbs (Fig. 4a). We estimated the volume of the cerebrum after separating it using the "draw tool" in the "surface view" window. The surface obtained was converted to a volume using the function "surface scan to volume". The volume of the cerebrum was then measured using the same two functions as for the overall brain and olfactory bulb volumes (Fig. 4a). When preserved, the petrosal lobules were re-segmented by creating a new material in the labelfield module (Fig. 4a). The anterior semicircular canal of the inner ear was used as a guide to isolate the petrosal lobule from the rest of the cerebellum (Bertrand et al. 2020; Lang et al. 2022). To generate the petrosal lobule volume, the same procedure was followed as for the above structures. The rhinal fissure was identifiable on the brain endocast surface of the studied specimens, which allowed us to measure the surface area of the neocortex. The neocortex was separated from the rest of the endocast using the same tools as for the cerebrum. One non-neocortical element, the superior sagittal sinus was included into the neocortical surface and not subtracted ("NS" in Bertrand et al. 2019). To quantify the surface of

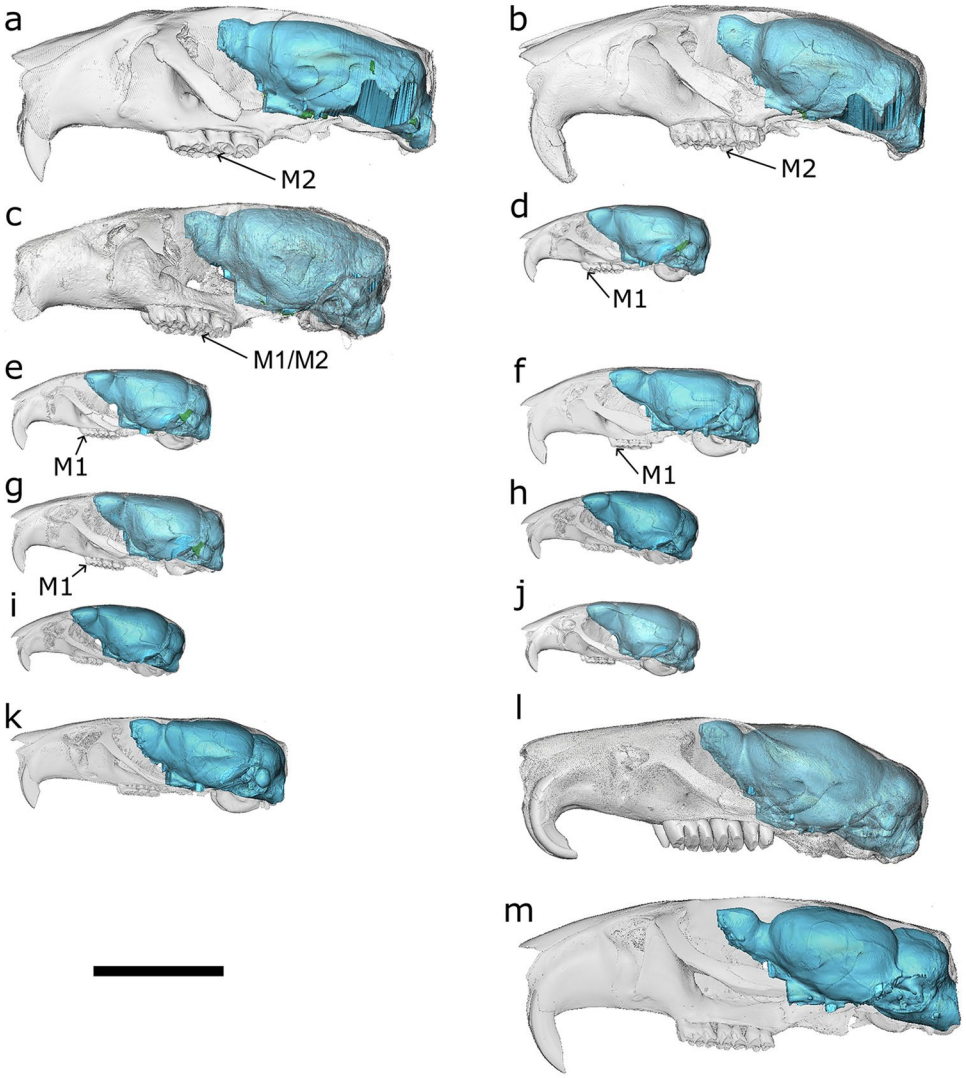

Fig. 3 Virtual brain endocast inside translucent skull of: **a.** *Canariomys bravoi*, IPS36548; **b.** *Canariomys bravoi*, TFM-CVF873; **c.** *Canariomys tamarani*, ZFMK 2010.308; **d.** *Arvicanthis niloticus*, MNHN-ZM-MO-1998-1113; **e.** *Arvicanthis niloticus*, MNHN-ZM-MO-2004-750; **f.** *Arvicanthis neumanni*, MNHN-ZM-MO-1978-195; **g.** *Arvicanthis abyssinicus*, MNHN-ZM-MO-1905–213 A; **h.** *Lemniscomys striatus*, MNHN-ZM-2008-6; **i.** *Pelomys fallax*, MNHN-ZM-MO-2007-1247; **j.** *Rhabdomys dilectus*, MNHN-ZM-2005-688; **k.** *Rattus rattus*, M−*443*; **l.** *Crateromys schadenbergi*, MNHN-ZM-MO-1897-414; **m.** *Phloeomys cumingi*, MNHN-ZM-AC-A7569. Scale bar equals 2 cm

the neocortex, the "extracted surface" and "surface area volume" functions were used (Fig. 4a). To obtain the surface of the paleocortex, we subtracted the surface of the neocortex from the cerebrum. The endocranial volume of both specimens of *Ca. bravoi* is slightly underestimated as the bullae and petrosal bones were missing from the specimens and therefore part of the cerebellum including the petrosal lobules could not be reconstructed.

Linear measurements (Table 2; Fig. 4b) were taken following Bertrand and Silcox (2016), using the 2D measurements function in Avizo. Ratios between different measurements were also obtained (Table 2). The measurements and ratios were represented as boxplots and also used as input for a principal component analysis (PCA). The PCA was performed with R v4.4.1 (R Core Team 2019) and R studio using the R packages "factoextra" (version 1.0.7) and "FactoMineR" (version 2.6). To visualize the results, we used the package "ggplot2" (3.4.0; Lê et al. 2008; Wickham 2009; Kassambara and Mundt 2020). We also estimated the body mass (BM) using the cranial length (CL) with the formula of Bertrand and Silcox (2016):

$$\mathrm{BM} = 10\mathrm{x}(((\mathrm{Log10}(\mathrm{CL}))\mathrm{x}3.9519) - 4.2316)$$

This method was chosen for its high determination coefficient ($r^2 = 0.96448$). The encephalization quotient (EQ) was calculated using the endocranial volume (EV) and the equation from Pilleri et al. (1984) that was specifically created for rodents (Table 3):

$$\mathrm{EQ} = \mathrm{EV}/(0.0997\mathrm{xBM}^{0.6419})$$

Institutional abbreviations ICP, Institut Català de Paleontologia Miquel Crusafont, Sabadell, Barcelona, Spain; **MNHN**, Muséum National d'Histoire Naturelle, Paris,

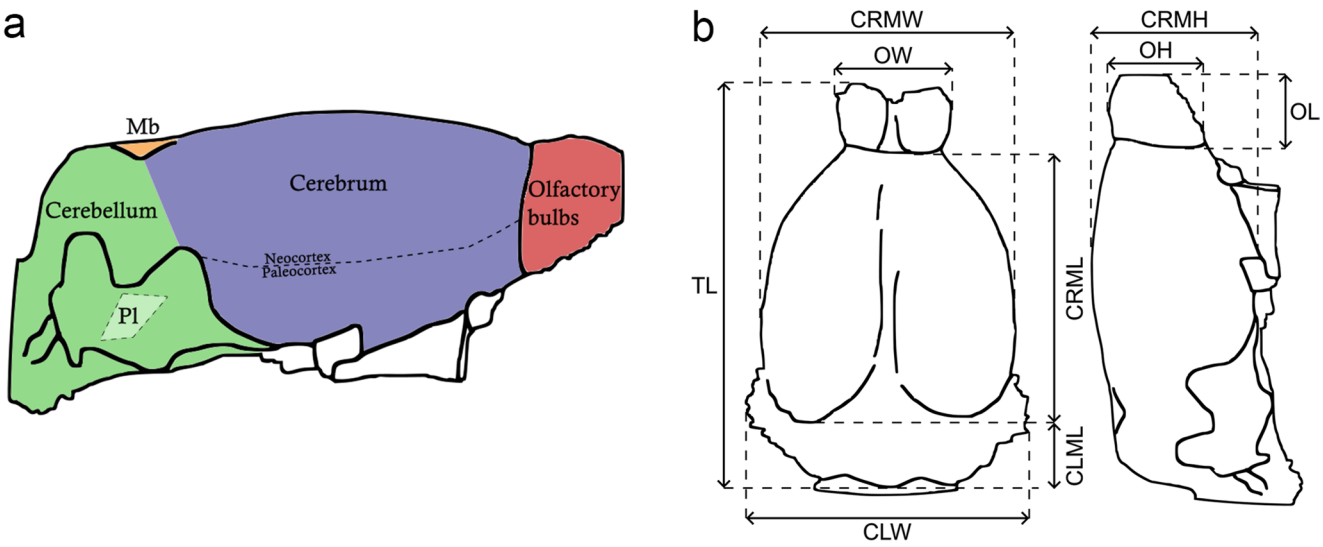

Fig. 4 Schematic rodent endocast based on *Canariomys bravoi* (IPS36548). **a.** different parts on the surface in lateral view; **b.** linear measurements taken in dorsal (left) and lateral (right) views, based on Bertrand et al. (2016: Fig. 5). Abbreviations: **CLML**, cerebellum maximal length; **CLW**, cerebellum width (without paraflocculi); **CRMH**, cerebrum maximal height; **CRML**, cerebrum maximal length; **CRMW**, cerebrum maximal width; **Mb**, midbrain; **OH**, olfactory bulbs height; **OL**, olfactory bulbs length; **OW**, olfactory bulbs width; **Pl**, petrosal lobule (the position is a hypothesis); **TL**, total endocast length

France; **MUNA**, Museo de la Naturaleza y el Hombre, Santa Cruz, Tenerife, Spain; **PACEA**, De la Préhistoire à l'Actuel: Culture, Environnement et Anthropologie; **ZFAK**, Zoologisches Forschungsmuseum Alexander Koenig, Bonn, Germany.

Descriptions and comparisons

Olfactory bulbs

Both olfactory bulbs are well preserved in all specimens, and these are always oval shaped. An anteroposterior longitudinal depression, corresponding to the superior olfactory sinus, is present between the bulbs and is wider mediolaterally in both *Ca. bravoi* specimens (IPS36548; TFMCVF873; Fig. 5a, b) and in *Ca. tamarani* (ZFMK 2010.308; Fig. 5c) compared to extant species. Compared to *Canariomys*, the cast of the superior olfactory sinus is narrower in *A. neumanni* (MNHN-ZM-MO-1978-195; Fig. 6b), *A. abyssinicus* (MNHN-ZM-MO-1905–213 A; Fig. 6c), and *A. niloticus* (MNHN-ZM-MO-1998-1113; Fig. 5d and MNHN-ZM-MO-2004-750; Fig. 6a). In contrast, there is no depression in *Ca. tamarani* (ZFMK 2010.308) and instead, a marked longitudinal elevation is present between the bulbs, which is continuous with the superior sagittal sinus on the cerebrum (Fig. 5c). This suggests that the superior olfactory sinus would have been more elevated in this specimen. The shape of each olfactory bulb in *Ca. bravoi* (IPS36548) is conical and the anterior parts of the bulbs are slightly larger and more laterally positioned anteriorly compared to the posterior parts (Fig. 5a). The other specimen of *Ca. bravoi* (TFMCVF873) also displays conical olfactory bulbs, but the overall shape of both bulbs taken together forms a rectangle with a longer anteroposterior length compared to the mediolateral width (Fig. 5b). The olfactory bulbs of *Ca. tamarani* are ovoid in shape (Fig. 5c). In contrast to *Canariomys*, the posterior aspect of the olfactory bulbs is wider than the anterior region in *A. neumanni* (Fig. 7b) and *A. niloticus* (MNHN-ZM-MO-1998-1113; Fig. 6d and MNHN-ZM-MO-2004-750; Fig. 6a), while the olfactory bulbs are more elongate anteroposteriorly and are even more rectangular in shape in *A. abyssinicus* (Fig. 6c).

Linear measurements indicate that the olfactory bulbs are relatively longer anteroposteriorly (18.04%) in *Ca. bravoi* (IPS36548) than in the other conspecific specimen TFMCVF873 (16.88%), but in the latter two specimens, the olfactory bulbs are shorter than those of all the other specimens in the comparative sample (20.85–25.97%; Table 2). *Canariomys bravoi* (IPS36548) has more mediolaterally expanded olfactory bulbs (45.78%) than those of all other compared specimens (34.54–38.08%; Table 2). Dorsoventrally, the olfactory bulbs have a lower height in *C. bravoi* (TFMCVF873; 47.68%) compared to all other specimens (52.41–57.83%; Table 2). *Canariomys bravoi* (TFMCVF873) has smaller olfactory bulbs anteroposteriorly and dorsoventrally than any of the other compared specimens (see values above; Table 2), but broader mediolaterally (37.77%; Table 2) than in *Ca. tamarani*, *A. neumanni*, *A. abyssinicus*, and *A. niloticus* (MNHN-ZM-MO-1998-1113; 34.54–35.98%). The

Table 2 Linear, surface and volumetric measurements taken on the different brain endocasts as well as the ratios calculated based on these measurements. The volume of the petrosal lobules of *Ca. bravoi* and the neocortical surface area of *Ca. tamarani* could not be measured (see text for more details)

Measurements	*Canariomys bravoi* (IPS36548)	*Canariomys bravoi* (TFMCVF873)	*Canariomys tamarani* (ZFMK 2010.308)	*Arvicanthis niloticus* (MNHN-ZM-MO-1998-1113)	*Arvicanthis niloticus* (MNHN-ZM-MO-2004-750)	*Arvicanthis neumanni* (MNHN-ZM-MO-1978-195)	*Arvicanthis abyssinicus* (MNHN-ZM-MO-1905–213 A)	*Lemniscomys striatus* (MNHN-ZM-2008-6)	*Pelomys fallax* (MNHN-ZM-MO-2007-1247)	*Rhabdomys dilectus* (MNHN-ZM-2005-688)	*Rattus rattus* (M-443)	*Crateromys schadenbergi* (MNHN-ZM-MO-1897-414)	*Phloeomys cumingi* (MNHN-ZM-AC-A7569)
Linear measurements (mm)													
Total endocast length (TL)	34.09	33.18	31.46	19.71	19.50	22.95	20.25	19.22	20.39	17.77	24.47	36.06	35.79
Cerebrum maximal width (CRMW)	21.82	21.13	21.19	12.84	12.70	13.50	13.09	11.94	12.98	10.93	16.21	21.05	22.14
Cerebrum maximal length (CRML)	22.04	21.13	19.77	11.50	11.12	12.90	11.30	11.30	12.19	9.46	13.23	19.67	21.44
Cerebrum maximal height (CRMH)	14.49	13.80	14.30	8.76	8.85	9.14	8.85	8.71	9.17	7.50	10.48	14.42	15.60
Cerebellum maximal length (CLML)	5.72	6.43	5.04	3.93	3.59	3.79	3.98	3.98	3.73	3.77	5.33	7.87	7.17
Cerebellum width (without petrosal lobules, CLW)	24.01	20.78	18.63	11.01	10.99	11.53	11.50	9.07	10.08	8.58	13.83	16.07	18.27
Olfactory bulb width (OW)	9.99	7.98	7.32	4.51	4.83	4.76	4.71	4.67	5.22	3.86	5.11	7.01	9.54
Olfactory bulb height (OH)	7.72	6.58	8.27	4.73	4.96	4.79	4.74	4.28	4.61	3.83	6.35	6.80	7.32
Olfactory bulb length (OL)	6.15	5.60	6.56	4.11	4.72	5.96	4.94	4.04	4.42	4.64	5.19	6.64	6.58
Ratio measurements (%)													
CRML/TL	64.65	63.68	62.84	58.35	57.03	56.21	55.8	58.79	59.78	53.24	54.07	54.55	59.91
CLML/TL	16.78	19.38	16.02	19.94	18.41	16.51	19.65	20.71	18.29	21.22	21.78	21.82	20.03
CLW/CRMW	110.04	98.34	87.92	85.75	86.54	85.41	87.85	75.96	77.66	78.5	85.32	76.34	82.52
OW/CRMW	45.78	37.77	34.54	35.12	38.03	35.26	35.98	39.11	40.22	35.32	31.52	33.3	43.09
OH/CRMH	53.28	47.68	57.83	54.00	56.05	52.41	53.56	49.14	50.27	51.07	60.59	47.16	46.92
OL/TL	18.04	16.88	20.85	20.85	24.21	25.97	24.4	21.02	21.68	26.11	21.21	18.41	18.39
Volumes (mm^3)													
Brain	6186.56	5456.54	5279.46	1059.44	1104.42	1415.73	1181.43	904.048	1207.56	680.567	2113.44	5403.25	5977.72
Olfactory bulbs	217.415	196.207	192.73	37.5649	46.808	72.8371	57.5692	40.1898	77.914	33.0157	89.7129	175.841	229.065
Petrosal lobules	-	-	37.7	10.75	9.71	12.26	10.95	9.956	12.98	8.546	19.81	8.36	26.64
Cerebrum	4099.51	3716.77	3759.69	723.863	748.059	934.981	802.148	662.891	894.314	472.292	1384.28	3700.32	4376.41
Surface areas (mm^2)													
Brain	2235.45	1979.79	2022.71	689.32	706.45	897.38	763.04	609.562	744.89	505.48	1110.39	2219.43	2153.23
Neocortex	681.35	666.9	-	219.687	223.66	254.275	229.26	221.557	259.62	175.294	333.548	674.11	748.78
Cerebrum	1436.14	1377.9	1311.95	441.963	443.528	533.61	467.899	400.148	495.354	322.228	694.21	1054.66	1449.77

Table 2 (continued)

Measurements	*Canariomys bravoi* (IPS36548)	*Canariomys bravoi* (TFMCVF873)	*Canariomys tamarani* (ZFMK 2010.308)	*Arvicanthis niloticus* (MNHN-ZM-MO-1998-1113)	*Arvicanthis niloticus* (MNHN-ZM-MO-2004-750)	*Arvicanthis neumanni* (MNHN-ZM-MO-1978-195)	*Arvicanthis abyssinicus* (MNHN-ZM-MO-1905–213 A)	*Lemniscomys striatus* (MNHN-ZM-2008-6)	*Pelomys fallax* (MNHN-ZM-MO-2007-1247)	*Rhabdomys dilectus* (MNHN-ZM-2005-688)	*Rattus rattus* (M-443)	*Crateromys schadenbergi* (MNHN-ZM-MO-1897-414)	*Phloeomys cumingi* (MNHN-ZM-AC-A7569)
Ratio volumes and surface areas to brain size (%)													
% Olfactory bulb volume	3.51	3.6	3.65	3.55	4.24	5.14	4.87	4.45	6.45	4.85	4.24	3.25	3.83
% Petrosal lobule volume	-	-	0.71	01.01	0.88	0.87	0.93	1.1	01.07	1.26	0.94	0.15	0.45
% Neocortex area	30.5	33.7	-	31.9	31.7	28.3	30	36.3	34.9	34.7	30	30.4	34.8
% Paleocortex area	33.76	35.91		32.25	31.12	31.13	31.27	29.30	31.65	29.07	32.48	17.15	32.56
Ratio volumes and surface areas to body mass (%)													
% Olfactory bulb volume	0.02	0.02	0.03	0.09	0.10	0.07	0.09	0.13	0.17	0.13	0.05	0.02	0.03
% Petrosal lobule volume	-	-	0.006	0.03	0.02	0.012	0.02	0.03	0.03	0.03	0.011	0.0008	0.0034
% Neocortex area	0.07	0.08	-	0.55	0.48	0.26	0.38	0.70	0.56	0.69	0.18	0.06	0.09
% Paleocortex area	0.08	0.09		0.56	0.47	0.28	0.39	0.56	0.51	0.58	0.20	0.03	0.09
Body mass (g)	995.13	806.33	586.64	39.66	46.4	98.38	60.66	31.82	46.58	25.27	180.35	1088.53	789.04

Table 3 Cranial length used to estimate body mass, estimated body mass, and encephalization quotient (EQ) for the different specimens

Species	Collection number	Cranial length (mm)	Endocranial volume (cm^3)	Body mass (g)	EQ Pilleri et al. (1984)
Canariomys bravoi	IPS36548	67.51	6.19	995.13	0.74
Canariomys bravoi	TFMCVF873	64.01	5.46	806.33	0.75
Canariomys tamarani	ZFMK 2010.308	59.06	5.28	586.64	0.88
Arvicanthis niloticus	MNHN-ZM-MO-1998-1113	29.87	1.06	39.66	1.00
Arvicanthis niloticus	MNHN-ZM-MO-2004-750	31.08	1.10	46.4	0.94
Arvicanthis neumanni	MNHN-ZM-MO-1978-195	37.59	1.42	98.38	0.75
Arvicanthis abyssinicus	MNHN-ZM-MO-1905–213 A	33.26	1.18	60.66	0.85
Lemniscomys striatus	MNHN-ZM-2008-6	28.25	0.90	31.82	0.98
Pelomys fallax	MNHN-ZM-MO-2007-1247	31.11	1.21	46.58	1.03
Rhabdomys dilectus	MNHN-ZM-2005-688	26.65	0.68	25.27	0.86
Rattus rattus	M-443	43.82	2.11	180.35	0.76
Crateromys schadenbergi	MNHN-ZM-MO-1897-414	69.06	5.40	1088.53	0.61
Phloeomys cumingi	MNHN-ZM-AC-A7569	63.66	5.98	789.04	0.83

olfactory bulbs of *Ca. tamarani* (ZFMK 2010.308) have the same relative anteroposterior length (20.85%; Table 2) as in *A. niloticus* (MNHN-ZM-MO-1998-1113; 20.85%) and are smaller than in *A. neumanni*, *A. abyssinicus*, and *A. niloticus* (MNHN-ZM-MO-2004-750; 24.21–25.97%). *Canariomys tamarani* also has smaller mediolaterally olfactory bulbs (34.54%) compared to all *Arvicanthis* species (35.12–38.03%; Table 2). The olfactory bulbs are positioned above the M2 in the two specimens of *Ca. bravoi* (Fig. 3a and b), above the M1 in *A. niloticus* (MNHN-ZM-MO-1998-1113 and MNHN-ZM-MO-2004-750), *A. neumanni*, and *A. abyssinicus*, and above the boundary between the M1 and the M2 in *Ca. tamarani* (Fig. 3c-g). The olfactory bulbs are not covered by the frontal lobes in any species (Figs. 7 and 8). The circular fissure is not well marked and appears to be more expanded anteroposteriorly in *Ca. bravoi* (IPS36548; Fig. 8a) than in TFMCVF873 (Fig. 8b). This feature is better defined in the other specimens and appears longer anteroposteriorly in *A. neumanni* compared to other species of *Arvicanthis* (Fig. 8b).

Cerebrum and midbrain

In dorsal view, the anteromedial boundaries of the cerebral hemispheres are not clearly defined in either of the *Ca. bravoi* (IPS36548; Fig. 5a and TFMCVF873; Fig. 5b) but they are visible on the other species and have a round outline (Figs. 5 and 6). However, the anterior boundaries are visible in lateral view in *Ca. bravoi* (TFMCVF873; Fig. 7b) as in the other specimens, but not in *Ca. bravoi* (IPS36548; Fig. 7a), in which they are only lightly marked (Figs. 7 and 8). In all species, the cerebral hemispheres are separated medially by the superior sagittal sinus (Figs. 5 and 6). The lateral borders of the anterior region of the cerebrum are convex in *Ca. bravoi* (TFMCVF873; Fig. 5b) and in *Ca. tamarani* (Fig. 5c), straight in *Arvicanthis* (Figs. 5d and 6a and b, and c), and intermediate in the other specimen of *Ca. bravoi* (IPS36548; Fig. 5a). In lateral view, a temporal fossa is visible in all species but is less marked in *Ca. bravoi* compared to *Arvicanthis* and to *Ca. tamarani* (Figs. 7 and 8). Sulci on the rodent brain are usually present when brains weight is over 5 g (Pilleri et al. 1984; Bertrand et al. 2016), and while *Canariomys* species have larger endocranial volumes (5.3–6.2 cm^3; Table 2) and should theorically have sulci, we do not see any sulci on any of the three specimens. The rhinal fissure separates the neocortex from the paleocortex and can be used to infer the degree of expansion of the neocortex (Jerison 2012; Long et al. 2015). The rhinal fissure is hard to distinguish in the two specimens of *Ca. bravoi* and is not visible in *Ca. tamarani* (Figs. 7 and 8).

In one specimen of *Ca. bravoi* (IPS36548), the limits between the cerebrum and the midbrain cannot be clearly distinguished, but in TFMCVF873, the midbrain is exposed (Fig. 5a, b). In *Ca. tamarani*, the midbrain appears to be fully covered by the confluence of sinuses and the vermis even though a thin indentation can be seen between both structures (Fig. 5c). In *A. neumanni* (Fig. 6b), *A. abyssinicus* (Fig. 6c), and *A. niloticus* (MNHN-ZM-MO-1998-1113; Fig. 5d and MNHN-ZM-MO-2004-750; Fig. 6a), the small patch of the midbrain is potentially visible, but the boundaries of this feature are hard to define with certainty. The pituitary gland (=hypophyseal fossa) is visible in *A. niloticus* (MNHN-ZM-MO-1998-1113) and *A. abyssinicus*, while in *Canariomys* and *A. neumanni*, this structure is not well demarcated (Figs. 9 and 10).

In terms of the linear measurements of the cerebrum, *Ca. bravoi* (IPS36548 and TFMCVF873) has a relatively longer cerebrum (63.68% and 64.65%) than *Ca. tamarani* (ZFMK 2010.308; 62.84%) and all *Arvicanthis* specimens (55.80–58.35.80.35%; Table 2). *Canariomys tamarani* has

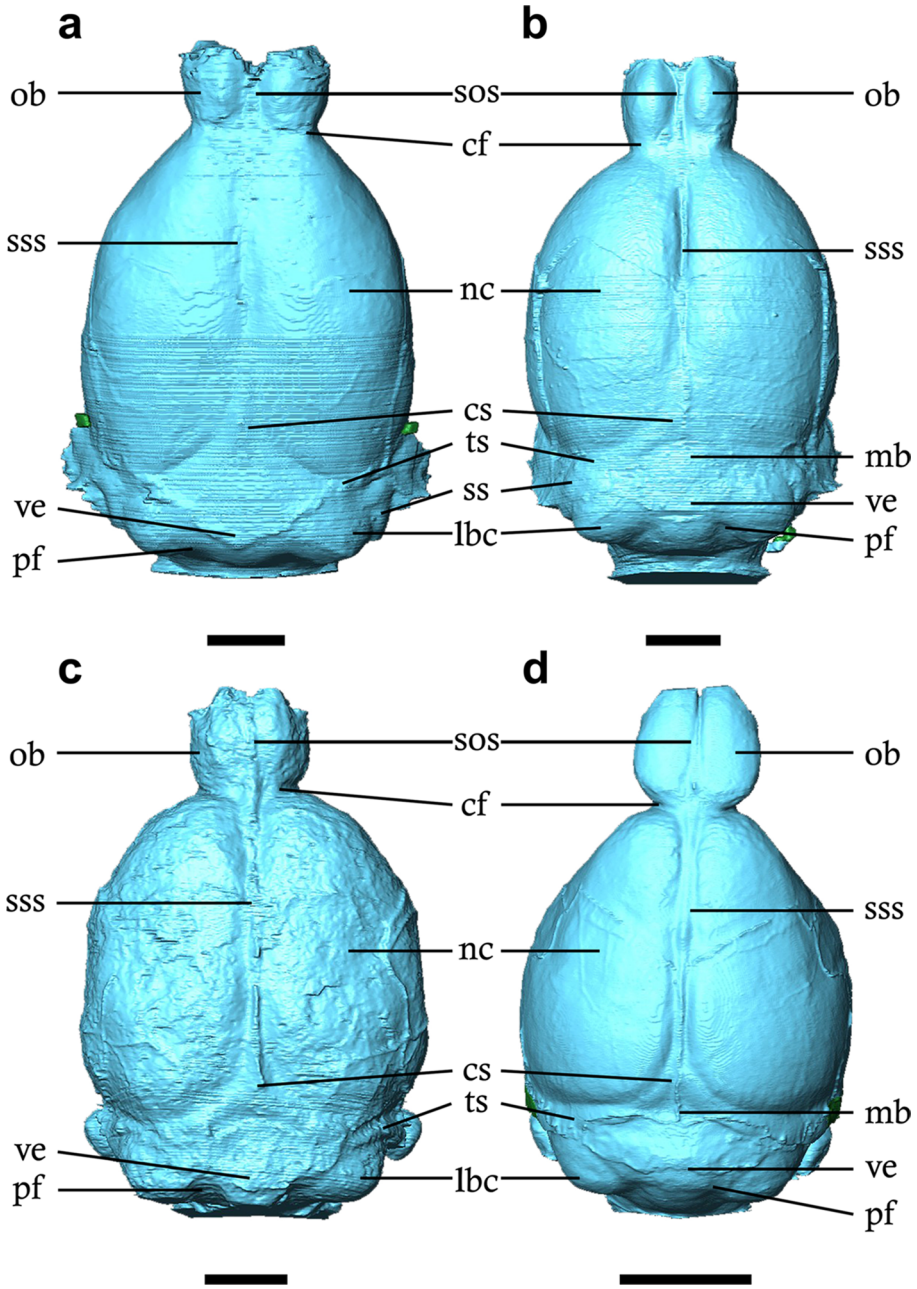

Fig. 5 Virtual endocasts in dorsal view. **a.** *Canariomys bravoi*, IPS36548; **b.** *Canariomys bravoi*, TFMCVF873; **c.** *Canariomys tamarani*, ZFMK 2010.308; **d.** *Arvicanthis niloticus*, MNHN-ZM-MO-1998-1113. Abbreviations: **cf**, circular fissure; **cs**, confluence of sinuses; **lbc**, lateral lobe of the cerebellum; **mb**, midbrain; **nc**, neocortex; **ob**, olfactory bulb; **pf**, paramedian fissure; **sos**, superior olfactory sinus; **sss**, superior sagittal sinus; **ss**, sigmoid sinus; **ts**, transverse sinus; **ve**, vermis. Scale bars equal 5 mm

the same cerebral width (21.19%) as *Ca. bravoi* (21.13% and 21.82%; Table 2). *Canariomys bravoi* (IPS36548) has a slightly longer cerebrum dorsoventrally (14.49 mm) compared to *Ca. bravoi* (TFMCVF873; 13.80 mm) and to *Ca. tamarani* (ZFMK 2010.308; 14.30 mm).

Cerebellum

Only part of the cerebellum is preserved in the studied *Ca. bravoi* specimens. The size of the cerebellum is challenging to assess because it is often covered at least partially by the cerebrum, therefore the values can be underestimated. For the studied sample, the cerebrum does not cover the medial region of the cerebellum but could potentially cover the lateral aspects of the cerebellum (Figs. 5 and 6). The vermis is visibly separated from the lateral lobes by the paramedian fissures, which are difficult to distinguish in *Ca. bravoi* (IPS36548; Fig. 5a) and are only visible posteriorly. For the other specimens, the vermis is more or less ovoid and its boundaries are more clearly demarcated, especially in *A. niloticus* (MNHN-ZM-MO-2004-750; Fig. 6a). The petrosal lobules are relatively bulbous in all species for which they were observed. They are not preserved in either of the specimens of *Ca. bravoi* because the petrosal region detached from the rest of the cranium (Figs. 7 and 8).

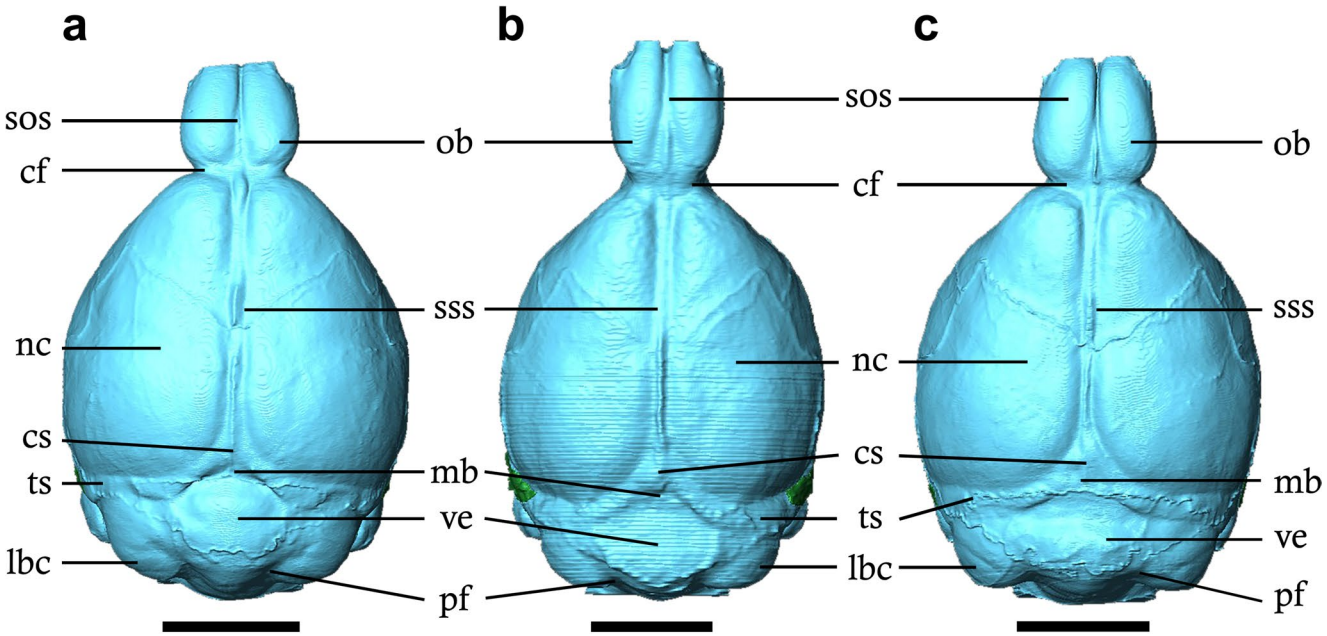

Fig. 6 Virtual endocasts in dorsal view. **a.** *Arvicanthis niloticus*, MNHN-ZM-MO-2004-750; **b.** *Arvicanthis neumanni*, MNHN-ZM-MO-1978-195; **c.** *Arvicanthis abyssinicus*, MNHN-ZM-MO-1905–213 A. Abbreviations: **cf**, circular fissure; **cs**, confluence of sinuses; **lbc**, lateral lobe of the cerebellum; **mb**, midbrain; **nc**, neocortex; **ob**, olfactory bulb; **pf**, paramedian fissure; **sos**, superior olfactory sinus; **sss**, superior sagittal sinus; **ts**, transverse sinus; **ve**, vermis. Scale bars equal 5 mm

Regarding linear measurements, *Ca. bravoi* (IPS36548) has a relatively longer mediolaterally cerebellum (110.04%) than *Ca. bravoi* (TFMCVF873; 98.34%; Table 2). This ratio is also higher in these specimens compared to *Arvicanthis* specimens (85.41–87.92%). This same ratio for *Ca. tamarani* (87.92%) is similar to *A. abyssinicus* (87.85%), but higher than for *A. niloticus* (MNHN-ZM-MO-1998-1113 and MNHN-ZM-MO-2004-750) and *A. neumanni* (Table 2). In terms of the anteroposterior length of the cerebellum, *Ca. bravoi* (IPS36548; 16.78%) resembles *Ca. tamarani* (16.02%) and *A. neumanni* (16.51%), but the ratio is lower compared to *Ca. bravoi* (TFMCVF873; 19.38%), *A. niloticus* (MNHN-ZM-MO-1998-1113, 19.84% and MNHN-ZM-MO-2004-750, 18.41%), and *A. abyssinicus* (19.65%; Table 2).

Brainstem and cranial nerves

The optic foramina, where the nerve II (optic) would have exited, are visible in all species. On both specimens of *Ca. bravoi* (IPS36548 and TFMCVF873), the nerve canals are not parallel and oriented laterally, while they are parallel in the other specimens and are oriented anteriorly (Figs. 9 and 10). The foramen rotundum, through which passes a branch of the trigeminal nerve V_2, is confluent with the sphenorbital fissure, which contains the ophthalmic vein, the nerves III (oculomotor), IV (trochlear), V_1 (ophthalmic branch of the trigeminal nerve), and VI (abducens). The foramen rotundum and sphenorbital fissure are merged in most rodents (Wahlert 1974; Bertrand et al. 2018). This configuration is present in all of our specimens. The nerve V_3 (mandibular), which is the largest branch of the trigeminal nerve, passes through the foramen ovale and the foramen ovale accessorius in many rodents (Wahlert 1974); however, there are exceptions (e.g., Bertrand et al. 2018). The foramen ovale accessorius is present in all extant species of the sample and in *Ca. tamarani*, but cannot be recognized in any of the *Ca. bravoi* specimens. Two canals for the branches of V_3, the buccinator and masseteric nerves, are visible on the extinct species. In *Ca. bravoi* (IPS36548 and TFMCVF873) and *Ca. tamarani*, this part of the V_3 forms a distinct canal that goes out of the endocranial cavity anteriorly to the alisphenoid canal (Fig. 9a-c). The configuration is different from all *Arvicanthis* species, which do not show any canal for the buccinator and masseteric nerves (Figs. 9 and 10).

The nerves VII (facial) and VIII (vestibulocochlear) are located inside the internal auditory meatus. They are not preserved in *Ca. bravoi* (Fig. 9a, b) because this region of the cranium is missing. In *Ca. tamarani* and extant species, both nerve casts can be identified (Figs. 9 and 10). The jugular foramen is the passageway for the jugular vein and cranial nerves IX (glossopharyngeal), X (vagus), and XI (spinal accessory), and is visible in the extant

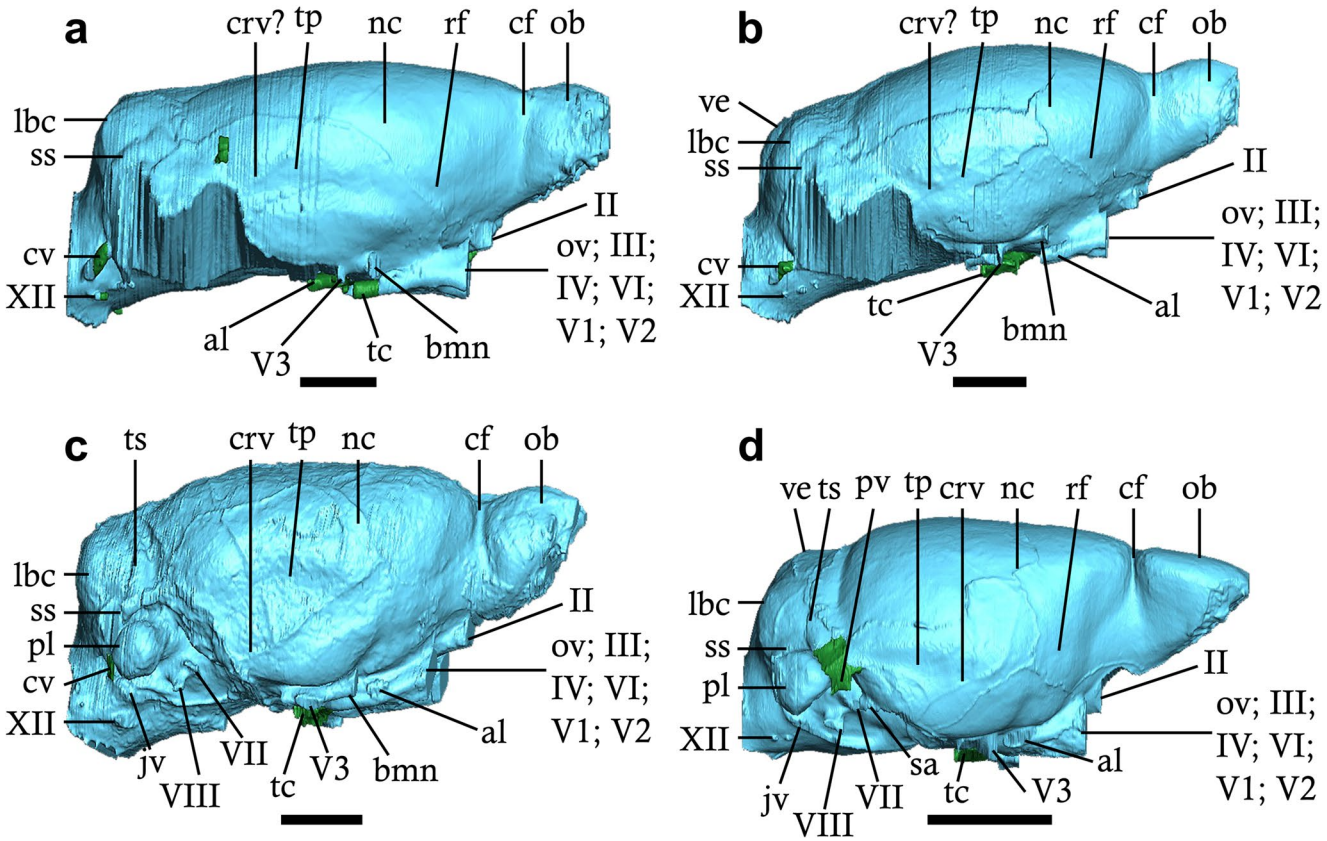

Fig. 7 Virtual endocast in right lateral view. **a.** *Canariomys bravoi*, IPS36548; **b.** *Canariomys bravoi*, TFMCVF873; **c.** *Canariomys tamarani*, ZFMK 2010.308; **d.** *Arvicanthis niloticus*, MNHN-ZM-MO-1998-1113. Abbreviations: **al**, alisphenoid canal; **bmn**, buccinator and masseteric nerves; **cf**, circular fissure; **crv**, caudal rhinal vein; **cv**, condyloid vessel; **jv**, jugular vein; **lbc**, lateral lobe of the cerebellum; **nc**, neocortex; **ob**, olfactory bulb; **ov**, ophthalmic vein; **pl**, petrosal lobule; **rf**, rhinal fissure; **sa**, stapedial artery; **ss**, sigmoid sinus; **tc**, transverse canal; **tp**, temporal fossa; **ts**, transverse sinus; **II**, optic nerve; **III**, oculomotor nerve; **IV**, trochlear nerve; **V1**, ophthalmic branch of the trigeminal nerve; **V2**, maxillary branch of the trigeminal nerve; **V3**, mandibular branch of the trigeminal nerve; **VI**, abducens nerve; **VII**, facial nerve; **VIII**, vestibulocochlear nerve; **XII**, hypoglossal nerve. Scale bars equal 5 mm

specimens. Because of incomplete preservation, the jugular foramen is not visible in *Ca. bravoi*, but can be seen in *Ca. tamarani* (Fig. 9a-c). The jugular foramen does not form a clear round foramen in extant species but resembles a fissure instead. The same foramen is very small in one specimen of *A. niloticus* (MNHN-ZM-MO-1998-1113; Fig. 9d) and much larger in the second one (MNHN-ZM-MO-2004-750; Fig. 10a). Posteriorly, the hypoglossal foramen contains the hypoglossal nerve (XII) and is visible on every specimen. The number of ramifications of the hypoglossal nerve varies. For the specimens of *Ca. bravoi* (IPS36548 and TFMCVF873), there are three ramifications (Fig. 9a, a), whereas there are two ramifications in *A. niloticus* (MNHN-ZM-MO-1998-1113; Fig. 9d and MNHN-ZM-MO-2004-750; Fig. 10a) and *A. abyssinicus* (Fig. 10c). One hypoglossal nerve is present in *A. neumanni* (Fig. 10b) and *Ca. tamarani* (ZFMK 2010.308; Fig. 9c), but breakage may have affected the preservation of the structure in the *Ca. tamarani* specimen.

Blood vessels

In dorsal view, the superior sagittal sinus is visible on every specimen. It separates the cerebral hemispheres and allows drainage of the blood of the dorsal venous system. The superior sagittal sinus is not well defined in the specimens of *Ca. bravoi* (IPS36548 and TFMCVF873; Fig. 5a, b) but is well demarcated and raised in the other species (Figs. 5 and 6). The superior sagittal sinus is connected with the transverse sinus by the confluence of sinuses positioned caudally to the cerebral hemispheres. The caudal rhinal vein is a ramification of the transverse sinus (Xiong et al. 2017). This vein is visible in the posterior part of the cerebrum in *Arvicanthis* (Figs. 7 and 8). The caudal rhinal vein of *Ca. bravoi* (IPS36548 and TFMCVF873) is positioned more dorsally on the temporal fossa than in *Ca. tamarani* and in the extant species. (Figures 7 and 8). In lateral view (Figs. 7 and 8), the sigmoid sinus is continuous with the transverse sinus and the internal jugular vein. The sigmoid sinus is more

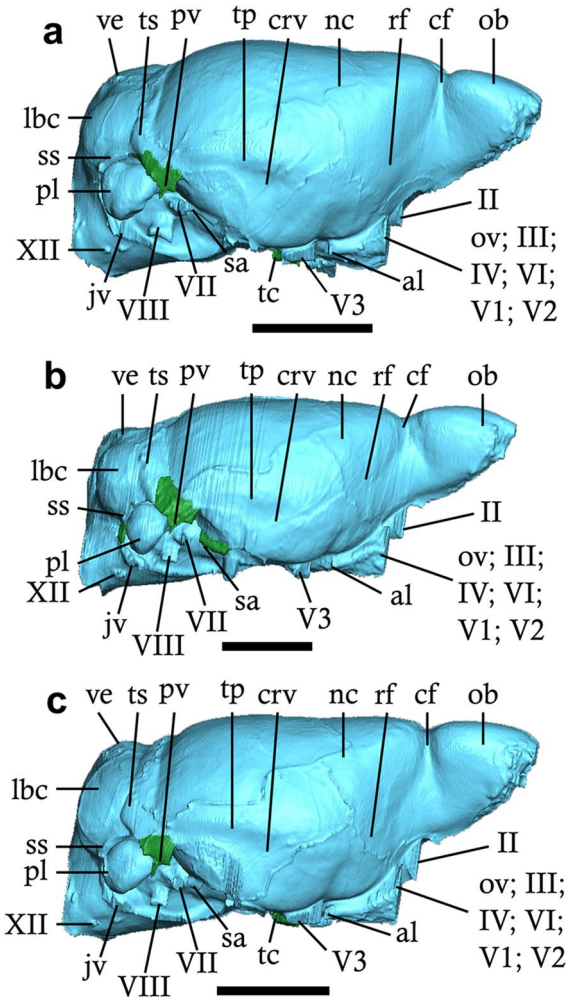

Fig. 8 Virtual endocast in right lateral view. **a.** *Arvicanthis niloticus*, MNHN-ZM-MO-2004-750; **b.** *Arvicanthis neumanni*, MNHN-ZM-MO-1978-195; **c.** *Arvicanthis abyssinicus*, MNHN-ZM-MO-1905–213 A. Abbreviations: **al**, alisphenoid canal; **cf**, circular fissure; **crv**, caudal rhinal vein; **jv**, jugular vein; **lbc**, lateral lobe of the cerebellum; **nc**, neocortex; **ob**, olfactory bulb; **ov**, ophthalmic vein; **pl**, petrosal lobule; **pv**, postglenoid vein; **rf**, rhinal fissure; **sa**, stapedial artery; **ss**, sigmoid sinus; **tc**, transverse canal; **tp**, temporal fossa; **ts**, transverse sinus; **ve**, vermis; **II**, optic nerve; **III**, oculomotor nerve; **IV**, trochlear nerve; **V1**, ophthalmic branch of the trigeminal nerve; **V2**, maxillary branch of the trigeminal nerve; **V3**, mandibular branch of the trigeminal nerve; **VI**, abducens nerve; **VII**, facial nerve; **VIII**, vestibulocochlear nerve; **XII**, hypoglossal nerve. Scale bars equal 5 mm

dorsally positioned, larger, and better defined in *Ca. bravoi* compared to all species of *Arvicanthis*. In *Ca. tamarani*, this sinus is similar in size to the one in *Ca. bravoi*, but it is positioned more ventrally than in *Ca. bravoi* (Fig. 7a-c). In *Arvicanthis*, the sigmoid sinus is positioned just dorsally to the petrosal lobules, abutting them, and is relatively smaller and not visible in dorsal view (Figs. 5, 6, 7 and 8). The sigmoid sinus runs anteroposteriorly and then dorsoventrally along the cerebellum and exits the cranium through the jugular foramen as the jugular vein (Wible 1990; Bertrand et al. 2024b). The other division of the transverse sinus is the capsuloparietal emissary vein, which exits the cranium more anteriorly via the postglenoid foramen as the postglenoid vein (Wible and Shelley 2020). Because of incomplete preservation, the postglenoid foramen and the cast of the capsuloparietal emissary vein are not visible in any of the *Canariomys* specimens (Fig. 7a-c). In extant species, the postglenoid foramen forms an opening and not a foramen, and the separation between the transverse sinus and the capsuloparietal emissary vein is not clear in these specimens (Figs. 8 and 9). The condyloid canal, carrying a vein, is connected to the sigmoid sinus and its content exits through the foramen magnum (Wible and Shelley 2020). This canal is visible in *Ca. bravoi* (IPS36548 and TFMCVF873), *A. neumanni*, and is only preserved on the right side of *Ca. tamarani* but is truly absent in the remaining extant species (Figs. 7 and 8).

One branch of the internal carotid artery is the stapedial artery (Wible 2022; Bertrand et al. 2024a). The cast of the stapedial artery is visible in all extant specimens (Figs. 7 and 8). In the two specimens of *Ca. bravoi*, the area that could have displayed the cast of the stapedial artery is not preserved (Figs. 7a and b and 9a and b). The area is preserved in *Ca. tamarani*, but the stapedial canal cannot be identified (Fig. 9c). Some bone degradation may be obscuring its presence. The alisphenoid canal carries the ramus inferior of the stapedial artery (Wible and Shelley 2020). The transverse canal is visible in all studied species, except in *A. neumanni* (Fig. 8b). This canal is well defined in the specimens of *Ca. bravoi* (IPS36548 and TFMCVF873), with the presence of the craniopharyngeal canal on the most ventral part in one of the specimens (IPS36548; Fig. 9a). The craniopharyngeal canal is also visible in *Ca. tamarani* (Fig. 9c) but absent in all *Arvicanthis* species (Figs. 9 and 10). For *Ca. tamarani*, *A. niloticus* (MNHN-ZM-MO-1998-1113 and MNHN-ZM-MO-2004-750), and *A. abyssinicus*, the transverse canal is overall less well defined. The transverse canal cannot be identified in *A. neumanni* even though the specimen appears well preserved (Figs. 9 and 10). The alisphenoid canal transmits internal artery and veins (Wahlert 1974) and is present in all species. The alisphenoid canal has an anteroposterior orientation similar to that of the cast of nerve V_2 in the two *Ca. bravoi* specimens (Fig. 9a, b). In contrast, the alisphenoid canal curves medially in *Ca. tamarani* (Fig. 9c) and in *A. niloticus* (MNHN-ZM-MO-1998-1113; Fig. 9d). In the remaining extant taxa, the alisphenoid canal curves laterally (Fig. 10).

Brain size and encephalisation quotient

The endocranial volumes are higher for all of the giant insular taxa compared to mainland species. *Rattus rattus* has a

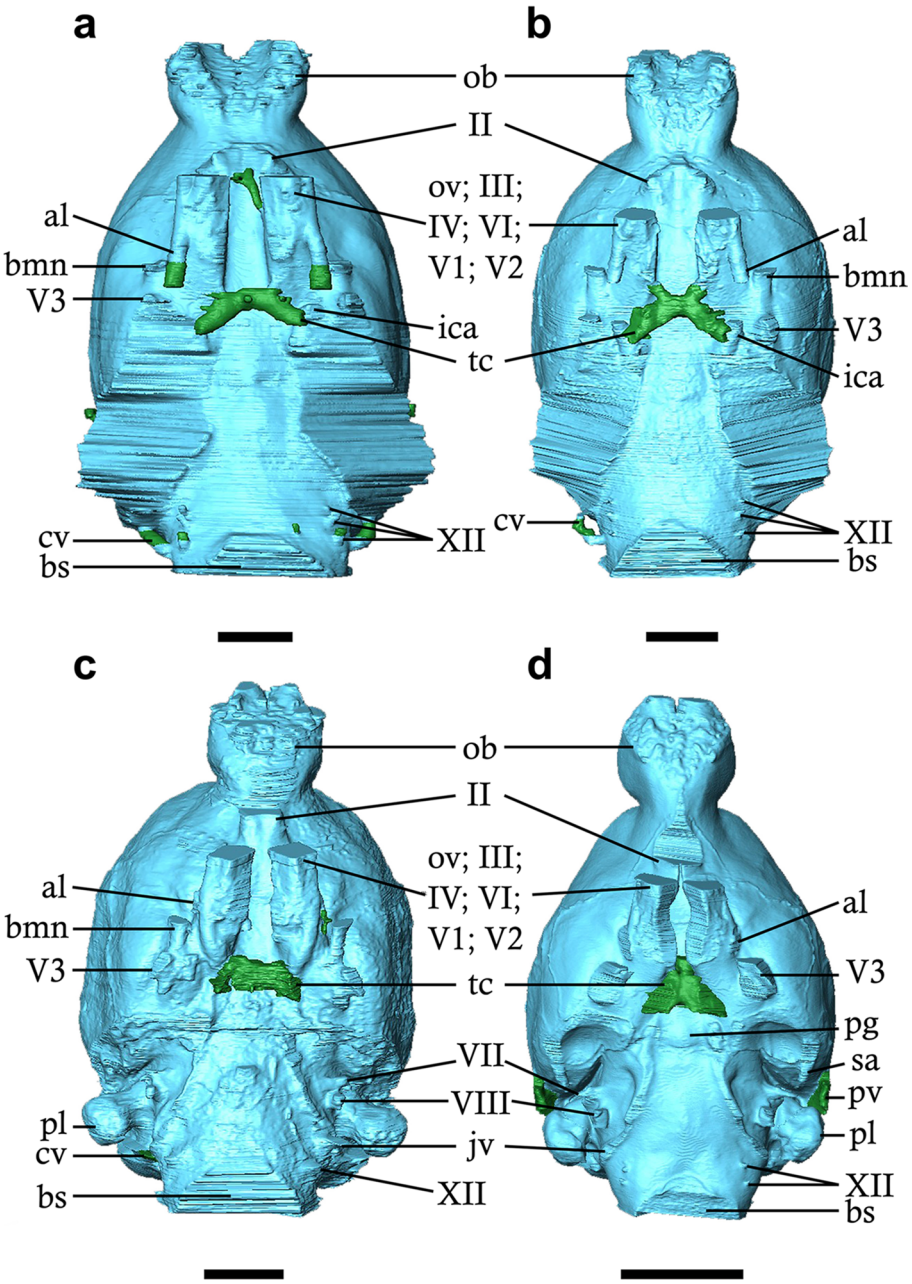

Fig. 9 Virtual endocasts in ventral view. **a.** *Canariomys bravoi*, IPS36548; **b.** *Canariomys bravoi*, TFMCVF873; **c.** *Canariomys tamarani*, ZFMK 2010.308; **d.** *Arvicanthis niloticus*, MNHN-ZM-MO-1998-1113. Abbreviations: **al**, alisphenoid canal; **bmn**, buccinator and masseteric nerves; **bs**, brainstem; **cv**, condyloid vessel; **ica**, internal carotid artery; **jv**, jugular vein; **ob**, olfactory bulb; **ov**, ophthalmic vein; **pl**, petrosal lobule; **pg**, pituary gland; **pv**, postglenoid vein; **sa**, stapedial artery; **tc**, transverse canal; **II**, optic nerve; **III**, oculomotor nerve; **IV**, trochlear nerve; **V1**, ophthalmic branch of the trigeminal nerve; **V2**, maxillary branch of the trigeminal nerve; **V3**, mandibular branch of the trigeminal nerve; **VI**, abducens nerve; **VII**, facial nerve; **VIII**, vestibulocochlear nerve; **XII**, hypoglossal nerve. Scale bars equal 5 mm

higher endocranial volume than the considered Arvicanthini species (Fig. 11a; Table 2). We assume that the endocranial volume of both *Ca. bravoi* specimens is underestimated because the bones associated with the petrosal region detached from the rest of the cranium. The results for the encephalization quotient (EQ; Fig. 11b) do not show the same pattern. Most extant species have EQs higher than 0.8. Within *Arvicanthis*, *A. niloticus* has a higher EQ (0.94 and 1.00) compared to all *Canariomys* specimens (0.74–0.88), is close to *L. striatus* (0.98) and *Pe. fallax* (1.03), while *A. neumanni* has a lower EQ than in the other *Arvicanthis* (0.75). Finally, *Cr. schadenbergi* displays the lowest EQ of the sample (0.61; Fig. 11b).

Olfactory bulb size

The overall range of the studied sample for the olfactory bulb volume ratio (Fig. 12a; Table 3) is between 3.25% for *Cr. schadenbergi* (lowest value) and 6.45% for *Pe. fallax* (highest value). *Canariomys bravoi* (3.51% and 3.60%) and *Ca. tamarani* (3.65%) have lower values than *A. niloticus* (3.55% and 4.24%). The other *Arvicanthis* species have relatively larger olfactory bulbs (5.14% for *A. neumanni* and 4.87% for *A. abyssinicus*). Except for *A. niloticus* (MNHN-ZM-MO-1998-1113), the endemic insular taxa have smaller olfactory bulbs than the mainland taxa and are close to the values of *Ca. bravoi*. Compared to body mass,

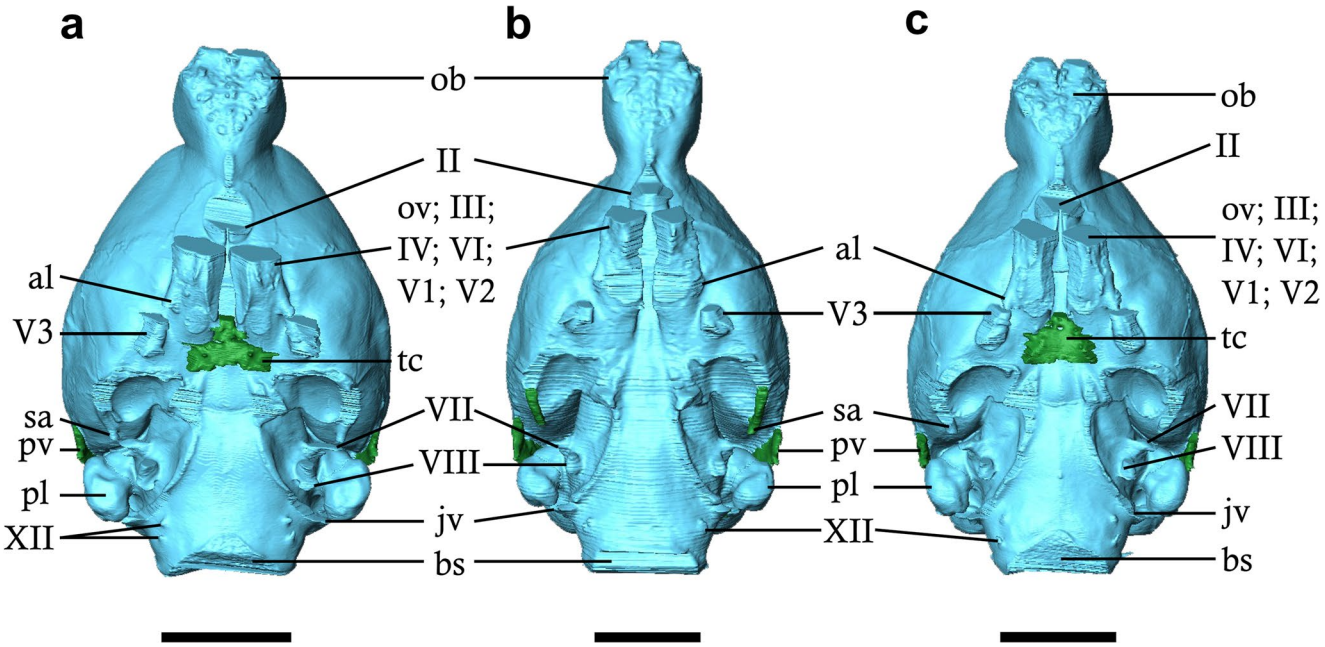

Fig. 10 Virtual endocasts in ventral view. **a.** *Arvicanthis niloticus*, MNHN-ZM-MO-2004-750; **b.** *Arvicanthis neumanni*, MNHN-ZM-MO-1978-195; **c.** *Arvicanthis abyssinicus*, MNHN-ZM-MO-1905–213 A. Abbreviations: **al**, alisphenoid canal; **bs**, brainstem; **jv**, jugular vein; **ob**, olfactory bulb; **ov**, ophthalmic vein; **pl**, petrosal lobule; **pg**, pituary gland; **pv**, postglenoid vein; **sa**, stapedial artery; **tc**, transverse canal; **II**, optic nerve; **III**, oculomotor nerve; **IV**, trochlear nerve; **V1**, ophthalmic branch of the trigeminal nerve; **V2**, maxillary branch of the trigeminal nerve; **V3**, mandibular branch of the trigeminal nerve; **VI**, abducens nerve; **VII**, facial nerve; **VIII**, vestibulocochlear nerve; **XII**, hypoglossal nerve. Scale bars equal 5 mm

all *Canariomys* specimens have lower ratios (0.02–0.03%) compared to any *Arvicanthis* specimens (0.07–0.09%). This is also the case for the two other island rodents, *Cr. schadenbergi* and *Ph. cumingi* that have lower ratios (0.02% and 0.03%) compared to their closest extant relative *Ra. rattus* (0.05%; Fig. 13a; Table 2).

Petrosal lobule size

Concerning the petrosal lobule ratio (Fig. 12b; Table 3), all Arvicanthini species have similar values, between 0.87% (*A. neumanni*) and 1.07% (*Pe. fallax*). The distribution is similar to the pattern observed for the olfactory bulbs (Fig. 12a). *Canariomys tamarani* has smaller petrosal lobules (0.71%) compared to *A. niloticus* (0.88% and 1.01%). Results show that insular taxa have smaller petrosal lobules, and *Cr. schadenbergi* and *Ph. cumingi* have the lowest values in the sample (Fig. 12b). In relation to body mass, the island rodents also have lower ratios than their closest extant mainland relatives (Fig. 13b; Table 2). *Canariomys tamarani* has a ratio of 0.006% compared to *Arvicanthis* (0.012% to 0.03%). The Philippine rodents *Cr. schadenbergi* and *Ph. cumingi* also have lower ratios (0.0008 and 0.0034%) compared to *Ra. rattus* (0.011%; Fig. 13b; Table 2).

Neocortical and paleocortical sizes

Regarding the neocortical surface area, the arvicanthines *Rh. dilectus* (34.68%), *Pe. fallax* (34.85%), and *L. striatus* (36.35%) show higher values (Fig. 12c) than *Arvicanthis niloticus* (31.87% and 31.66%), *A. abyssinicus* (30.05%) and *A. neumanni* (28.34%). When comparing the insular murines from the Philippines, *Cr. schadenbergi* (30.37%) has a lower value than *Ph. cumingi* (34.77%; Fig. 12c). Both specimens of *Ca. bravoi* (30.48% and 33.69%) overlap with extant arvicanthines. Finally, *Ra. rattus* (30.04%) is close to *Cr. schadenbergi* and *A. abyssinicus* (Fig. 12c). The neocortical surface area for *Ca. tamarani* could not be estimated because of the lack of preservation of the rhinal fissure. Compared to body mass, the neocortex of *Canariomys* represents a lower ratio (0.07–0.08%) in comparison to *Arvicanthis* (0.26–0.55%). Similar results are found when comparing *Cr. schadenbergi* and *Ph. cumingi* (0.06–0.09%) with *Ra. rattus* (0.18%; Fig. 13c; Table 2). Concerning the paleocortical surface area, both specimens of *Ca. bravoi* have the highest percentage ratio (33.76% and 35.91%) in relation to endocranial size compared to the rest of the sample (17.15–32.56%). The lowest value corresponds to *Cr. schadenbergi* (Fig. 12d; Table 2). The range of variation for

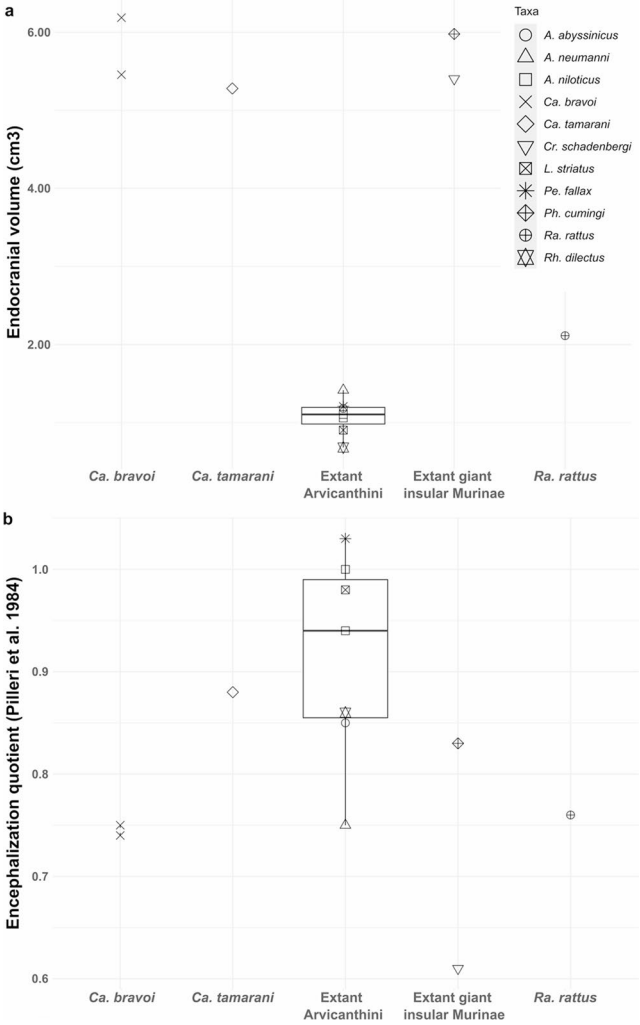

Fig. 11 Boxplots for *Canariomys* and other murines for **a.** Endocranial volume (cm^3); **b.** Encephalization quotient. The extremities of the boxplot correspond to the minimum and maximum values for all boxplots

Arvicanthis is relatively narrow (31.12–32.25%) compared to the neocortical surface area (Fig. 12d; Table 2). Compared to body mass, the paleocortical surface area ratio is lower in both specimens of *Ca. bravoi* (0.08–0.09%) and in the two other insular species *Cr. schadenbergi* and *Ph. cumingi* (0.03–0.09%) in comparison to the mainland taxa (0.20–0.58%; Fig. 13d; Table 2).

Principal component analysis

Based on the linear measurements, the first two principal components of the PCA explain 94.7% of the total variation (Fig. 14a; Online Resource 1: Table S2). All variables contribute positively to PC1 (Online Resource 2: Fig. S1a), which suggests that this component can be interpreted as a size axis. The results of this PCA show a group with the giant insular taxa displaying the highest values of all measurements, and a second group including mainland taxa exhibiting lower values (Fig. 14a). Because this PCA only shows differences in size, we used ratios of these measurements to characterize actual proportional differences (Table 2).

The PCA of the ratio measurements (Fig. 14b) shows a different pattern. The first two principal components explain 74.7% of the total variation (PC1: 48.3% and PC2: 26.4%; Online Resource 1: Table S3). For PC1, the variables CLW/TL, CRML/TL and OW/CRMW have strong positive loading values (Fig S1b). In PC1, the specimens with high positive PC values tend to have relatively longer cerebellum width (CLW), cerebrum maximal length (CRML), and olfactory bulb width (OW; Online Resource 2: Fig S1b). For PC2, OH/CRMH and OL/TL have positive loading values and CLML/TL has a negative loading value, so specimens with high PC values tend to have relatively longer olfactory bulb height (OH) and olfactory bulb length (OL) but smaller cerebellum maximal length (CLML). The reverse is true for specimens with negative values on PC2 (Fig. 14b). The specimens of *Arvicanthis* species are close to one another in the morphospace, suggesting the same ratios and limited variation within this genus (Fig. 14b). We note that *Ca. bravoi*, *Cr. schadenbergi*, and *Ca. tamarani* have positive values along the PC1, meaning a relatively longer cerebrum, wider cerebellum and wider olfactory bulbs as compared the other taxa (Fig. 14b; Online Resource 2: Fig S1b). Also, *Ca. bravoi* has a relatively longer cerebrum and broader olfactory bulbs dorsoventrally in comparison to *Ca. tamarani* on PC1 (Fig. 14b; Online Resource 2: Fig S1b). On PC1, *Ca. tamarani* is closer to *Arvicanthis* than *Ca. bravoi*, while on PC2, this species shows the highest value among all taxa (Fig. 14b). Overall, this position in the morphospace suggests that *Ca. tamarani* has relatively mediolaterally smaller olfactory bulbs and an anteroposteriorly shorter cerebrum than *C. bravoi*. Additionally, *Ca. tamarani* has a cerebellum that is mediolaterally longer, but anteroposteriorly shorter compared to other taxa.

Discussion

Intra- and interspecific variation in *Canariomys* and close relatives

In terms of morphological variation, we notice a higher intraspecific variation within *Ca. bravoi* compared to the variation within *A. niloticus*. Additionally, there is also more variation within the genus *Canariomys* than within *Arvicanthis* (Online Resource 1: Table S4). Notably, the shape and proportions of the olfactory bulbs, as well as the cast of the superior olfactory sinus size, vary substantially between *Ca.*

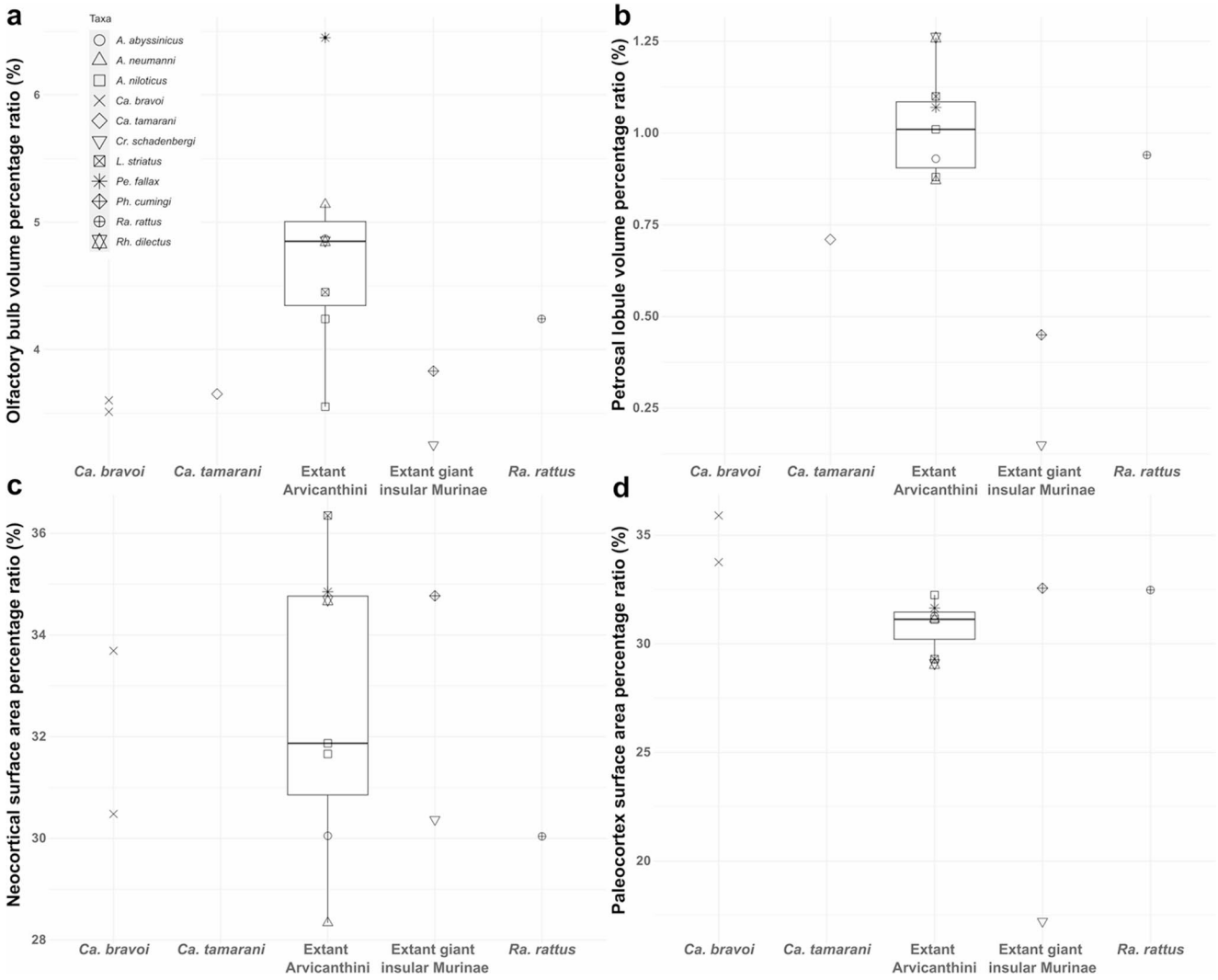

Fig. 12 Boxplots of different brain region ratios in relation to brain size for *Canariomys* and other murines (%). **a.** Olfactory bulb volume ratio; **b.** Petrosal lobule volume ratio; **c.** Neocortical surface area ratio; **d.** Paleocortex surface area ratio. The extremities of the boxplot correspond to the minimum and maximum values in all boxplots

bravoi and *Ca. tamarani*. In contrast, *Arvicanthis* displays more uniform olfactory bulbs and superior olfactory sinus sizes (Table S4). The same is true for other casts of sinuses and nerves, including the number of hypoglossal foramina, the definition of the transverse canal, and the orientation of the alisphenoid canal between *Ca. bravoi* and *Ca. tamarani* (Online Resource 1: Table S4). Regarding size variation, our results show that the relative size of the brain of the three specimens of *Canariomys* are within the range of *Arvicanthis*; however, we observe that *Canariomys* has a lower EQ than its closest extant relative, *A. niloticus*. Our results differ from Blanco-Lapaz (2005, 2007), who did not notice a decrease in relative brain size in *Canariomys* in comparison to a sample of different murid genera, including *Arvicanthis*. In his work, there were no specific comparisons made with either *Arvicanthis* or *A. niloticus*.

Phenotypic variability has been shown to potentially be stronger in island settings (Baeckens and Van Damme 2020). Therefore, we expect a higher variability in *Ca. bravoi* than in *A. niloticus* and by extension, a higher variation within the genus *Canariomys* than within the genus *Arvicanthis*. First, there is overall more relative variation in the linear measurements in *Ca. bravoi* in comparison to the *A. niloticus* (Online Ressources 2: Fig. S2a). A similar pattern is also present for the neocortical surface area ratios (Fig. 12c). This is also the case between *Canariomys* and *Arvicanthis* with the linear and volumetric relative measurements (Online Ressources 2: Figs. S2b; Fig. 12). Surprisingly, the relative size variation of the olfactory bulbs is much lower in *Ca. bravoi* in comparison to *A. niloticus*. The same is true and even more pronounced when comparing both genera with each other (Fig. 12a). High variability

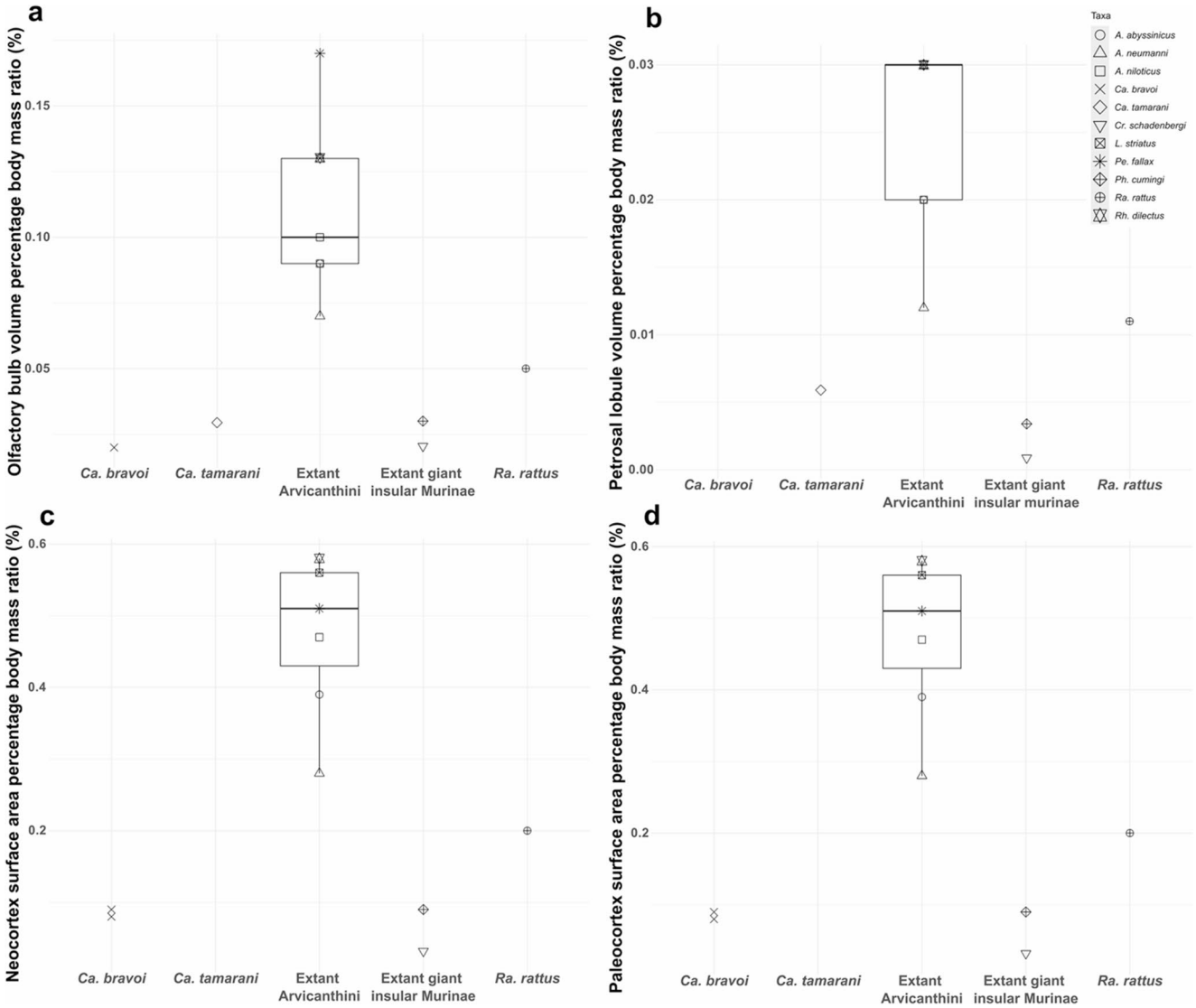

Fig. 13 Boxplots of different brain region ratios in relation to body mass for *Canariomys* and other murines (%). **a.** Olfactory bulb volume ratio; **b.** Petrosal lobule volume ratio; **c.** Neocortical surface area ratio; **d.** Paleocortex surface area ratio. The extremities of the boxplot correspond to the minimum and maximum values in all boxplots

could be the result of low selective pressures in *Arvicanthis* for olfaction, while there may have been more selective pressures on the olfactory bulbs of *Canariomys*. This may suggest that the sense of smell became less crucial and was negatively selected in *Canariomys.* However, we note some limitations to these interpretations. We only have two data points for *Ca. bravoi* and one for *Ca. tamarani*. Therefore, we remain cautious about our findings related to intraspecific, interspecific, and intrageneric variations. Additionally, the specimens of *Ca. bravoi* come from different localities that might differ in age (i.e., Cueva de la Palomas and Cueva del Viento). The age of Cueva de las Palomas is unknown, but could be equivalent to the age of Cueva del Viento, which is ca. 12,000 cal BP.

We observe no clear morphological differences between the two specimens of *A. niloticus*, except for the hypophyseal fossa that is more expanded in one of them. *Arvicanthis niloticus* and *A. abyssinicus*, which can be discriminated using genetic data (Bryja et al. 2019; Renom et al. 2021), exhibit very similar brain endocranial morphologies. Based on previous work (Monadjem et al. 2015; Wilson et al. 2017), A. *abyssinicus* is endemic to Ethiopia and can only be distinguished from *A. niloticus* by chromosome number. Regardless of its geographical distribution, morphology cannot be used to discriminate between these two species. In contrast, *A. neumanni* appears to have a different morphology of the olfactory bulbs, an absence of transverse canal, and only one hypoglossal nerve. Additionally, *A. neumanni*

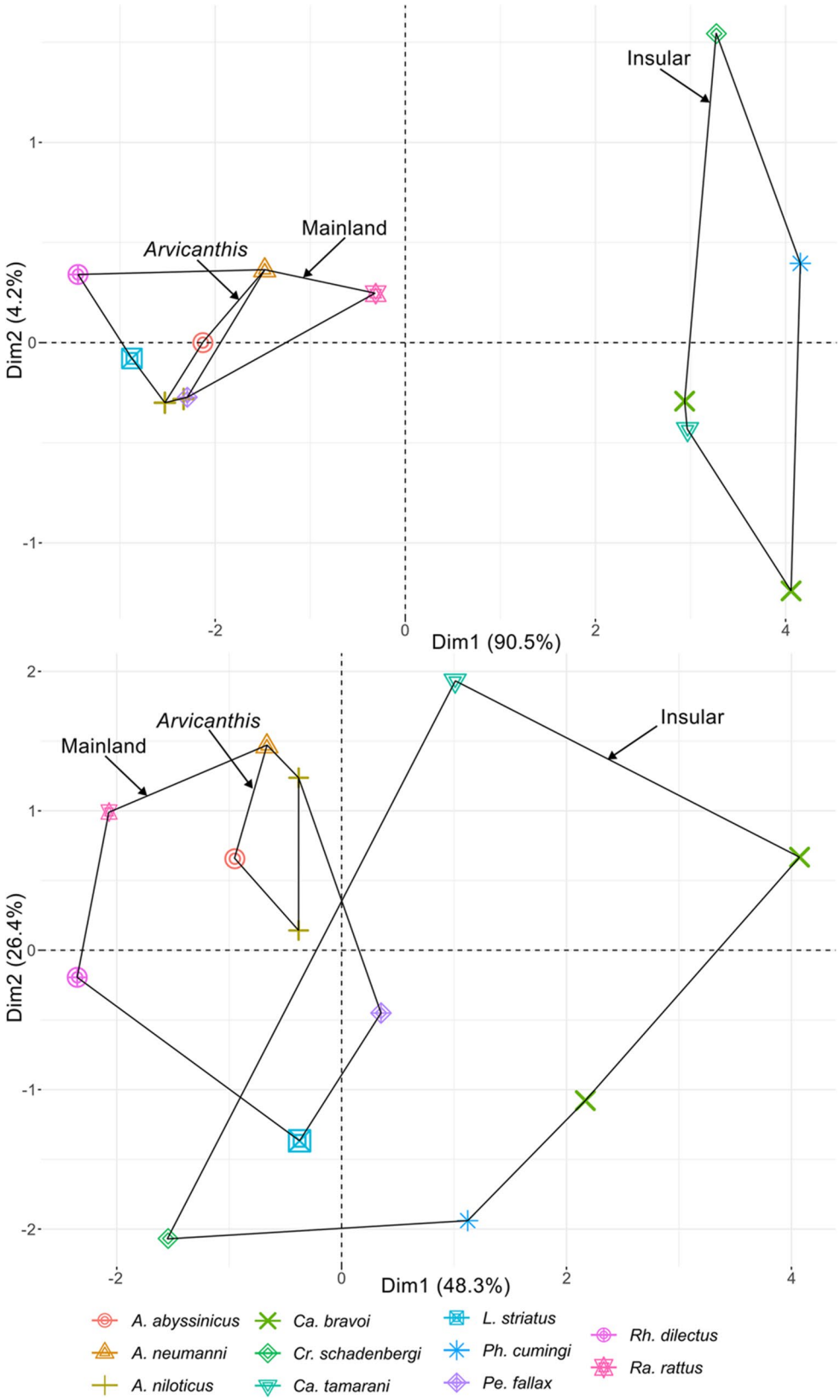

Fig. 14 **a.** Plot of the first two principal components based on the endocranial linear measurements. **b.** Plot of the first two principal components based on the ratio of endocranial linear measurements. For *Ca. bravoi* and *A. niloticus*, the average was calculated and is represented by a larger symbol for both taxa on the plot

has the smallest neocortical surface area ratio of all the considered *Arvicanthis* species (Fig. 12c). The olfactory bulb volume ratio of *A. neumanni* is much higher than in both specimens of *A. niloticus* (Fig. 12a). *Arvicanthis neumanni* was misidentified as *A. niloticus* by Michaux et al. (2012), but our results for the brain endocast show evidence that *A. neumanni* belongs to a distinct species. Overall, the brain endocast could potentially be used as a diagnostic criterion to differentiate *A. neumanni* from *A. niloticus* in future studies. However, our sample size is limited, and this hypothesis should be tested with a higher number of specimens.

Canariomys tamarani presents morphological states of the brain endocast that are either similar to *Ca. bravoi* or to *Arvicanthis*. For instance, similarly to *Arvicanthis*, the olfactory bulbs are ovoid, the anteromedial boundaries of the cerebral hemispheres are round, the superior sagittal sinus is clearly defined, the transverse canal is not well defined, and the caudal rhinal vein and sigmoid sinus are ventrally positioned in comparison to *Ca. bravoi*. In contrast, morphological features that are only present in specimens of *Canariomys* include a wider superior olfactory sinus, a canal of the buccinator and masseteric nerves, and a larger sigmoid sinus (Online Resource 1: Table S4). Finally, the position of the olfactory bulbs in relation to the cheek toothrow is intermediate in *Ca. tamarani* (M1-M2), while *Ca. bravoi* (M2) and *Arvicanthis* (M1) present one of the two conditions (Online Resource 1: Table S4). From these results, we can hypothesize that *Ca. tamarani* might display an overall less derived morphology than *Ca. bravoi.* This is in agreement with data from dental morphology, which show that *Ca. tamarani* is more similar to *A. niloticus* than *Ca. bravoi*, the latter showing a more derived morphology (Casanovas-Vilar and Luján 2022). *Canariomys tamarani* may be a more basal species to *Ca. bravoi*, but this hypothesis needs to be rigorously tested, and unfortunately, doing so will be challenging since no information on the age of *Ca. tamarani* is available. It is also possible that the two species derived from different dispersal events, in which case inclusion within the same genus would be questionable (see Casanovas-Vilar and Luján 2022).

Brain regions and reduction of senses in *Canariomys*

Our results show that the relative brain size of *Ca. bravoi* is in the low range of *Arvicanthis* and only overlaps with *A. neummani*. *Canariomys tamarani* has a larger relative brain size than *Ca. bravoi*, but it is still smaller than the two species of *A. niloticus*. Since *Canariomys* is more closely related to *A. niloticus* than any of the other *Arvicanthis* species, we can hypothesize that there is a decrease in relative brain size in *Canariomys.* Previous studies have shown that insular species generally display a reduction in relative brain size compared to mainland relatives (Köhler and Moyà-Solà 2004; Palombo et al. 2008; Quintana et al. 2011; Csiki-Sava et al. 2018; Lyras 2018; Liakopoulou et al. 2024). Because the brain is already metabolically expensive to maintain, the energy that is not used by the brain can be re-allocated to the rest of the body. This might in turn lead to an increase in body size and a decrease in relative brain size. A similar pattern has been observed in early placental mammals that survived the end-Cretaceous extinction (Bertrand et al. 2022).

Additionally, when compared to *Arvicanthis*, the olfactory bulbs and the paleocortex of *Ca. bravoi* are relatively smaller compared to both brain and body sizes, and the olfactory bulbs are relatively smaller to the body size for *Ca. tamarani* (Table 2). Reduction in olfaction has been found in other insular mammals with choanae (posterior nasal aperture) being reduced in the giant insular rabbit *Nuralagus rex* from Minorca (Quintana et al. 2011). This reduction in olfaction could be related to a decrease in predation threat because of the increase in body mass of *Canariomys* (Fig. 15). Previous work has shown that small mammals rely on olfactory cues to detect the presence of predators (Brinkerhoff et al. 2005). In Gran Canaria, fossils from four different birds of prey have been found including *Buteo buteo* (Common buzzard), *Accipiter nisus* (Eurasian sparrowhawk), *Falco tinnunculus* (Common kestrel), *Tyto* sp. (Owl). On Tenerife, only the remains of *B. buteo* and *A. nisus* have been recovered (Sánchez Marco, 2010). These different predatory birds do not hunt prey that are more than 250 g (Perrin 1982; Korpimäki 1985; Selås 1993; Selås et al. 2007), which is well below the body mass of *Canariomys*.

We also considered diet as a factor that may have impacted the size of the olfactory bulbs in *Canariomys*. The diet of *Arvicanthis* is currently debated. Based on stomach content and faecal matter, *Arvicanthis* may ingest 5% to 40% of animal matter and therefore has been described as omnivore (Taylor and Green 1976; Delany and Monro 1986; Rabiu and Fisher 1989). More recently, two studies concluded that *Arvicanthis* had a stricter herbivorous diet based on stomach content and isotope analyses (Taylor and Green 1976; Bergstrom 2013). It is likely that the diet of *Arvicanthis* changes seasonally and that plants might be favoured during the dry season, while animal matter is consumed in the rainy season (Wilson et al. 2017). Regarding the diet of *Canariomys*, based on microwear analysis, mandibular geometric morphometrics, $\delta^{15}N$ and $\delta^{13}C$ stable isotopes, *Ca. bravoi* preferentially consumed C_3 vegetation, most likely leaves, fruits or seeds (Bocherens et al. 2003, 2006; Firmat et al. 2010). On the other hand, the relatively high $\delta^{15}N$ indicates that *Canariomys* likely ate a significant proportion of animal matter (Crowley et al. 2019). Based on these different studies, a dietary shift does not appear to have occurred between *Arvicanthis* and *Canariomys.*

Fig. 15 Life reconstruction of the rodent *Canariomys* on the island of Tenerife made by Jesús Gamarra. *Mus musculus*, which likely coexisted with *Canariomys* (Rando et al. 2014), is included for scale. The reconstruction of *Canariomys* is based on the skull and skeleton published by Michaux et al. (2012)

The covering of the midbrain has been studied in many mammals (e.g., Edinger 1964) and its degree of exposure has been linked to the development of the neocortex, which occurs independently in different clades (Bertrand et al. 2022; Dozo et al. 2023). In rodents and in other mammals, as the neocortex expands, it tends to cover the midbrain (e.g., Bertrand et al. 2017). Therefore, the midbrain is covered in many recent mammals but exposed in numerous extinct species (e.g. Orliac et al. 2012; Bertrand et al. 2019, 2020, 2024a, b, 2025; López-Torres et al. 2023). Based on previous work, the common ancestor of rodents likely had an exposed midbrain (Meng et al. 2003; Bertrand et al. 2016, 2019). This caudal expansion of the neocortex over the midbrain has been interpreted as being specifically linked to the expansion of the occipital lobe where the visual cortex is located (Silcox et al. 2010). Therefore, mammals with expanded caudal neocortex may have had enhanced vision. However, it is important to note that there is no easy way to verify whether that is the case since endocasts only preserve the surface of the brain. It is possible that other regions of the brain may have expanded, leading to the occipital lobe to become more caudally positioned in specimens with covered midbrain.

Canariomys bravoi (TFMCVF873) has an exposed midbrain, while this structure is almost completely covered by the confluence of sinuses (and neocortex) in *Ca. tamarani* and in all specimens belonging to *Arvicanthis.* The condition in *Ca. bravoi* (IPS36548) cannot be determined for certainty. An exposed midbrain can have significant paleoecological implications, but because the colliculi are not visible (Edinger 1964), it is difficult to justify for a sensory specialization. The neocortical size of *Ca. bravoi* is within the range of variation of *Arvicanthis* but relative to body mass, it represents a smaller proportion (Table 2). Therefore, it is possible that a reduction of the neocortex occurred in *Ca. bravoi* (no neocortical data could be generated for *Ca. tamarani*) and the visibility of the midbrain is a byproduct and does not represent any sensory specialization. More specimens of *Canariomys* are required to better understand the midbrain exposure variation in this genus. Previous

research has found intraspecific variation in two different euarchontogliran groups: the plesiadapiform *Microsyops* and the ischyromyid rodent *Ischyromys* (Silcox et al. 2010; Bertrand and Silcox 2016).

Relatively large petrosal lobules (in relation to both brain and body size) have been interpreted to have a role in maintaining eye and head movements during locomotion and are present in more active and visually oriented animals, such as arboreal squirrels and terrestrial/scansorial caviomorphs (e.g., Bertrand et al. 2017, 2021; Fernández Villoldo et al. 2023). In contrast, relatively smaller petrosal lobules in aplodontiids have been interpreted as a specialization to a more fossorial lifestyle (slower locomotion; Bertrand et al. 2018, 2021), but also in Euarchontoglires more generally (Lang et al. 2022) and in subterranean mammals (Goyens et al. 2022). Our results show that the island species *Ca. tamarani* (no data for *Ca. bravoi*) and the Philippines rodents *Cr. schadenbergi* and *Ph. cumingi* have relatively smaller petrosal lobules (in relation to both brain and body size; Table 2) in comparison to *Rattus* and *Arvicanthis*. In terms of locomotor behaviour, *Cr. schadenbergi* and *Ph. cumingi* have both been described as arboreal, but overall, very little is known about their ecology (Oliver et al. 1993). *Phloeomys cumingi* can live in seriously degraded habitats, including predominantly agricultural and pastureland. *Crateromys schadenbergi* is less tolerant to environmental changes and is restricted to forested habitats (Oliver et al. 1993). The locomotor behaviour of *Ca. tamarani* is not known, but *Ca. bravoi* may have been able to climb and dig based on analyses of postcranial remains (Michaux et al. 2012). Even if we cannot be certain of their locomotor behavior, we may hypothesize that, based on past studies cited above, these different island rodents moved more carefully through their preferred substrate based on the relatively small petrosal lobule size. In the future, we plan to survey a wider range of island species to see whether this pattern subsists as this is the first study that incorporates the size of petrosal lobules in island species.

Models for brain evolution in insular mammals

In mammals and birds, relatively larger brains have been linked to greater "behavioral flexibility" and may represent an advantage to respond to environmental changes or new environments (Schuck-Paim et al. 2008; Sol et al. 2008; Sol 2009). However, placental mammals that radiated after the end-Cretaceous extinction show a faster rate of evolution in body mass than in brain size, leading to a decrease in relative brain size (Bertrand et al. 2022). The same authors hypothesized that because of low competition for resources during the Early Paleocene, increasing brain complexity was not necessary and could have even been detrimental. Similarly, here, we do not observe an increase in relative brain size in *Canariomys*. Additionally, *Ca. bravoi* has a relative brain size in the very low range of variation of *Arvicanthis* and both *Canariomys* species have lower EQs than their sister-clade *A. niloticus*. As previously discussed, this decrease in relative brain size might be linked to a decrease in the olfactory bulbs and potentially of the paleocortex that is also linked to the sense of smell. Indeed, the cerebrum volume in relation to body mass in *Canariomys* is lower than in *A. niloticus* (Table 2). In relation to body mass, the neocortex and the paleocortex sizes of *Canariomys* are both below those of *A. niloticus*. A low level of interspecific competition has been found on islands (Lomolino 2005). This may have favoured the evolution of forms that did not require significant behavioural adaptations and may have led to a decrease in brain regions related to olfaction and the integration of senses.

The Philippines rodents *Cr. schadenbergi* and *Ph. cumingi* also show a reduction in the same brain regions (olfactory bulbs, petrosal lobules, neocortex, and paleocortex) in comparison to *Rattus*, which would suggest an "island effect" on the brain of rodents. Similar patterns have been observed in other mammals. *Nuralagus rex*, an insular endemic lagomorph from Late Neogene karstic deposits of Minorca (Balearic Islands, Spain), shows a reduction of the tympanic bullae, orbits, choanae, and braincase (Quintana et al. 2011). These authors concluded that this giant lagomorph had a relatively smaller brain compared to its mainland relatives, which they interpreted as a reduction of associated sensory organs responsible for audition and vision. The same pattern may be present in the endemic bovid *Myotragus*, from the Plio-Pleistocene deposits of Majorca (Spain), and the Cretan deer *Candiacervus*. They both show a reduction of relative brain size of 45–50% in *Myotragus balearicus* (Köhler and Moyà-Solà 2004; but only 17% when compared to contemporaneous Late Miocene taxa Liakopoulou et al. 2024) and 13–22% in *Candiacervus* compared to extant close relatives (Palombo et al. 2008). This relative reduction of the brain was accompanied by a reduction of the orbits and motor-related brain areas. These neurosensory changes have been associated with predator-free insular environments (Palombo et al. 2008). Some other studies have found different results. Despite finding a reduction in relative brain size in the islander Cretaceous multituberculate, *Litovoi tholocephalos* from Romania, relatively larger olfactory bulbs and petrosal lobules were found compared to its mainland relatives, which was interpreted as an increase in sensory acuity (Csiki-Sava et al. 2018). However, no comparisons were made in relation to body mass. In contrast, Lyras (2018) showed that dwarf elephants (e.g., the Middle Pleistocene Sicilian dwarf elephant, *Palaeoloxodon falconeri*) and hippos displayed an increase in EQ compared to closely related mainland taxa. This study did not specifically look at sensory changes.

Conclusions

In this study, we described the brain endocasts of two specimens of *Ca. bravoi* and one of *Ca. tamarani* from the Canary Islands. We made comparisons with three different species of *Arvicanthis*, its closest continental relative. We show that the intraspecific endocranial morphological and size variation within the insular *Canariomys* is higher than within the mainland *Arvicanthis*, although the specimens belonging to *Ca. bravoi* might be of different ages and more data are needed to confirm this hypothesis. If these specimens are of similar age, this would support previous studies that have shown that phenotypic variability is higher on islands (Baeckens and Van Damme 2020). We find evidence for differentiating *A. neumanni* from *A. niloticus* based on endocranial anatomy. As previous studies have struggled in finding morphological differences between these two species (Michaux et al. 2012), we suggest that using endocranial features may help in diagnosing morphologically similar species. Our results show that *Ca. tamarani* could have retained more plesiomorphic features present in *Arvicanthis* compared to *Ca. bravoi*, as previously suggested based on dental morphology (Casanovas-Vilar and Luján 2022).

We found that the relatively small size of the olfactory bulbs in both species of *Canariomys* and paleocortex in *Ca. bravoi*, might be related to a decrease in predation pressure on the island in comparison to mainland *Arvicanthis*. The birds of prey on Tenerife and Gran Canaria are species that eat smaller preys (Sánchez Marco 2010). Based on our results, the common ancestor of *Canariomys* and *Arvicanthis* likely had a covered midbrain and *Ca. bravoi* (TFMCVF873) displays a derived condition that might be due to the reduction of the neocortex. We also find that all island rodents including *Canariomys*, *Cr. schadenbergi* and *Ph. cumingi* show a reduction in the relative size of the petrosal lobules, which indicates that these mammals may move more carefully in their preferred substrate. Previous research has shown that relatively small petrosal lobules are found in species that move slowly or live partially or fully underground (Bertrand et al. 2021; Goyens et al. 2022; Lang et al. 2022; Fernández Villoldo et al. 2023). In the future, one of our goals is to increase the sample of island species to see if this is a prevalent pattern and look for possible interpretations.

Our results show that no increase in relative brain size in *Canariomys* was linked to living in this new insular environment in comparison to its mainland relative *Arvicanthis*. Previous work has hypothesized that increase in brain size and "behavioral flexibility" occurred as a response to a change in environmental conditions or the exposure to a new environment (Schuck-Paim et al. 2008; Sol et al. 2008; Sol 2009). Instead, we find a decrease in relative brain size that might be linked to low competition for resources, as previously found for placental mammals that survived the end-Cretaceous extinction (Bertrand et al. 2022). This decrease resulted from a decrease in diverse senses via the reduction in specific brain regions (i.e., olfactory bulbs, petrosal lobules, paleocortex, and neocortex). Previous studies on other island mammals have also found a reduction in various senses, including vision and audition as well as in locomotor functions (Köhler and Moyà-Solà 2004; Palombo et al. 2008; Quintana et al. 2011). Ultimately, we add new evidence to suggest that living on islands has a strong influence on the morphology of the brain and on the size of different brain regions and associated behaviours.

Supplementary Information The online version contains supplementary material available at https://doi.org/10.1007/s10914-025-09785-0.

Acknowledgements This work was supported by the Beatriu de Pinós Programme funded by the Direcció General de Recerca de la Generalitat de Catalunya (General Directorate for Research in the Government of Catalonia) and managed by AGAUR, expedient number: 2021 BP 00042 to OCB; This work is part of R + D + I project PID2020-117289GBI00 funded by the Agencia Estatal de Investigación of the Ministerio de Ciencia e Innovación (MCIN/AEI/10.13039/501100011033/) and also supported by the Ayuda RYC2023-042630-I financiada por MICIU/AEI /10.13039/501100011033 y por el FSE+ to OCB. Research has also been supported by the Generalitat de Catalunya/CERCA Programme. OCB and ICV are members of the consolidated research group 2021 SGR 00620 of the Agència de Gestió d'Ajuts Universitaris i de Recerca of the Generalitat de Catalunya and we thank the 'Miquel Crusafont Program of predoctoral contracts' for supporting JG. The new CT scans were funded by the EVODIBIO team (A. Le Cabec) and the ENDORAT project funded by the PACEA laboratory under the ANCOR funding call to AS and OCB. We thank V. Colin and C. Denys (MNHN) for the loan of the specimens and L. Courtenay who brought back the specimens to the MNHN. We thank N. Vanderesse for the CT scans of the MNHN specimens. We also thank R. Lebrun for the CT scan of *Canariomys bravoi* (TFMCVF873) and *Ca. tamarani*, and to À. H. Luján (ICP) for the scan of the *Canariomys bravoi* (IPS36548) type specimen. We thank the Graduate Program ARCHEO and the ERASMUS program for their support that allowed FV to work on his master's project in Spain. AS benefited from the scientific framework of the University of Bordeaux's IdEx "Investments for the Future" program/GPR "Human Past". We would like to thank two anonymous reviewers for their helpful suggestions and comments, the editor-in-chief D. Croft and associate editor M. Arnal for their editorial work.

Author contributions This work corresponds to the Master dissertation of FV at the Institut Català de Paleontologia Miquel Crusafont. **Conceptualization: ** FV, OCB, AS, ICV; **Data Curation: ** FV, OCB, AS, ICV; **Formal Analysis: ** FV; **Funding Acquisition: ** OCB, AS, ICV; **Investigation: ** FV, OCB, AS, ICV; **Methodology: ** FV, OCB, AS, ICV; **Supervision** OCB, AS, ICV; **Visualization** FV, JG; **Writing – Original Draft Preparation** FV; **Writing – Review & Editing: ** FV, OCB, AS, ICV, JG.

Funding Open Access funding provided thanks to the CRUE-CSIC agreement with Springer Nature.

Data availability All data generated or analysed during this study are included in this published article and its supplementary information files.

Declarations

Data archiving statement The code to reproduce the analyses is on the Github Repository: https://github.com/Flavien-VINCENT/Canariomys-brain-evolution, and the brain virtual endocasts for the different specimens are accessible in MorphoSource: https://www.morphosource.org/projects/000709494?locale=en.

Competing interests Two authors OCB and ICV are associate editors for the Journal of Mammalian Evolution, but they were not involved in the evaluation of this manuscript.

References

Aghová T, Kimura Y, Bryja J, Dobigny G, Granjon L, Kergoat GJ (2018) Fossils know it best: using a new set of fossil calibrations to improve the temporal phylogenetic framework of murid rodents (Rodentia: Muridae). Mol Phylogenet Evol 128:98–111. https://doi.org/10.1016/j.ympev.2018.07.017

Baeckens S, Van Damme R (2020) The island syndrome. Curr Biol 30(8):R338-R339. https://doi.org/10.1016/j.cub.2020.03.029

Bate DMA (1909) Preliminary note on a new Artiodactyle from Majorca, *Myotragus balearicus*, gen. et sp. nov. Geol Mag 6(9):385–388. https://doi.org/10.1017/S0016756800124665

Benítez-López A, Santini L, Gallego-Zamorano J, Milá B, Walkden P, Huijbregts MAJ, Tobias JA (2021). The island rule explains consistent patterns of body size evolution in terrestrial vertebrates. Nat Ecol Evol 5(6):768–786. https://doi.org/10.1038/s41559-021-01426-y

Benoit J, Crumpton N, Mérigeaud S, Tabuce R (2013) A memory already like an elephant's? The advanced brain morphology of the last common ancestor of Afrotheria (Mammalia). Brain Behav Evol 81(3):154–169. https://doi.org/10.1159/000348481

Benton MJ, Csiki Z, Grigorescu D, Redelstorff R, Sander PM, Stein K, Weishampel DB (2010) Dinosaurs and the island rule: Tthe dwarfed dinosaurs from Haţeg Island. Palaeogeogr Palaeoclimatol Palaeoecol 293(3–4):438–454. https://doi.org/10.1016/j.palaeo.2010.01.026

Bergstrom BJ (2013) Would East African savanna rodents inhibit woody encroachment? Evidence from stable isotopes and microhistological analysis of feces. J Mammal 94(2):436–447. https://doi.org/10.1644/12-MAMM-A-146.1

Bertrand OC, Silcox MT (2016) First virtual endocasts of a fossil rodent: *Ischyromys typus* (Ischyromyidae, Oligocene) and brain evolution in rodents. J Vertebr Paleontol 36(3): e1095762. https://doi.org/10.1080/02724634.2016.1095762

Bertrand OC, Schillaci MA, Silcox MT (2016) Cranial dimensions as estimators of body mass and locomotor habits in extant and fossil rodents. J Vertebr Paleontol 36(1):e1014905 https://doi.org/10.1080/02724634.2015.1014905

Bertrand OC, Amador-Mughal F, Silcox MT (2017) Virtual endocast of the early Oligocene *Cedromus wilsoni* (Cedromurinae) and brain evolution in squirrels. J Anat 230(1):128–151. https://doi.org/10.1111/joa.12537

Bertrand OC, Amador-Mughal F, Lang MM, Silcox MT (2018) Virtual endocasts of fossil Sciuroidea: Brain size reduction in the evolution of fossoriality. Palaeontology 61(6):919–948. https://doi.org/10.1111/pala.12378

Bertrand, O.C., Amador-Mughal, F., Lang, M.M. & Silcox, M.T. (2019). New virtual endocasts of Eocene Ischyromyidae and their relevance in evaluating neurological changes occurring through time in Rodentia. J Mamm Evol 26:345–371. https://doi.org/10.1007/s10914-017-9425-6

Bertrand OC, Shelley SL, Wible JR, Williamson TE, Holbrook L T, Chester SGB, Butler IB, Brusatte SL (2020). Virtual endocranial and inner ear endocasts of the Paleocene 'condylarth' *Chriacus*: New insight into the neurosensory system and evolution of early placental mammals. J Anat 236(1):21–49. https://doi.org/10.1111/joa.13084

Bertrand OC, Püschel HP, Schwab JA, Silcox MT, Brusatte SL (2021) The impact of locomotion on the brain evolution of squirrels and close relatives. Commun Biol 4:460. https://doi.org/10.1038/s42003-021-01887-8

Bertrand OC, Shelley SL, Williamson TE, Wible RJ, Chester JGB (2022) Brawn before brains in placental mammals after the end-Cretaceous extinction. Science 376(6588):80–85. https://doi.org/10.1126/science.abl5584

Bertrand OC, Jiménez LM, Shelley SL, Wible JR, Williamson TE, Meng J, Stephen LB (2024a) The virtual brain endocast of *Trogosus* (Mammalia, Tillodontia) and its relevance in understanding the extinction of archaic placental mammals. J Anat 244:1–21. https://doi.org/10.1111/joa.13951

Bertrand OC, Lang MM, Ferreira JD, Kerber L, Kynigopoulou Z, Silcox MT (2024b) The virtual brain endocast of *Incamys bolivianus*: Insight from the neurosensory system into the adaptive radiation of South American rodents. Pap Palaeontol 10(3):e1562. https://doi.org/10.1002/spp2.1562.

Bertrand OC, Michaud M, Kirk EC (2025) How the neurosensory system provides clues for the adaptive radiation of mammals. In: Krubitzer LA (ed.) Evolution of Nervous Systems in Mammals. Evolution of Nervous Systems, 3rd edn, vol. 2. Elsevier, Amsterdam. https://doi.org/10.1016/B978-0-443-27380-3.00019-1 Accessed 10 11 2025.

Biddick M, Hendriks A, Burns KC (2019) Plants obey (and disobey) the island rule. Proc Natl Acad Sci USA 116(36):17632–17634. https://doi.org/10.1073/pnas.1907424116

Blanco-Lapaz A (2005) Estudio de *Canariomys bravoi* (Crusafont y Petter, 1964) del Plio-Cuaternario de Las Islas Canarias. Un ejemplo de evolución insular. In: Meléndez G, Martínez-Pérez C, Ros S, Botella H, Plasencia P (eds) Miscelánea Paleontológica. Semin Paleontol Zaragoza 6:187–204

Blanco-Lapaz A (2007) Estudi de l'encéphal a *Canariomys bravoi* (Rodentia, Muridae) del Plio-Holocè de Tenerife. Dissertation, Universitat Autònoma de Barcelona.

Boback SM (2003) Body size evolution in snakes: evidence from island populations. Copeia 2003(1):81–94. https://doi.org/10.1643/0045-8511(2003)003[0081:BSEISE]2.0.CO;2

Bocherens H, Michaux J, Billiou D, Castanet J, Garcia-Talavera F (2003) Contribution of collagen stable isotope biogeochemistry

to the paleobiology of extinct endemic vertebrates from Tenerife (Canary Islands, Spain). Isot Environ Health Stud 39(3):197–210. https://doi.org/10.1080/1025601031000113574

Bocherens H, Michaux J, Talavera FG, Van Der Plicht J (2006) Extinction of endemic vertebrates on islands: The case of the giant rat *Canariomys bravoi* (Mammalia, Rodentia) on Tenerife (Canary Islands, Spain). C R Palevol 5(7):885–891. https://doi.org/10.1016/j.crpv.2006.04.001

Boyer AG, Jetz W (2010) Biogeography of body size in Pacific Island birds. Ecography 33(2):369–379. https://doi.org/10.1111/j.1600-0587.2010.06315.x

Brinkerhoff RJ, Haddad NM, Orrock JL (2005) Corridors and olfactory predator cues affect small mammal behavior. J Mammal 86(4):662–669. https://doi.org/10.1644/1545-1542(2005)086[0662:CAOPCA]2.0.CO;2

Bromham L, Cardillo M (2007) Primates follow the 'island rule': implications for interpreting *Homo floresiensis*. Biol Lett 3(4):398–400. https://doi.org/10.1098/rsbl.2007.0113

Brown P, Sutikna T, Morwood MJ, Soejono RP, Jatmiko, Wayhu Saptomo E, Awe Due R, (2004) A new small-bodied hominin from the Late Pleistocene of Flores, Indonesia. Nature 431(7012):1055–1061. https://doi.org/10.1038/nature02999

Bryja J, Colangelo P, Lavrenchenko LA, Meheretu Y, Šumbera R, Bryjová A, Verheyen E, Leirs H, Castiglia R, (2019) Diversity and evolution of African Grass Rats (Muridae: *Arvicanthis*) From radiation in East Africa to repeated colonization of northwestern and southeastern savannas. J Zool Syst Evol Res 57(4):970–988. https://doi.org/10.1111/jzs.12290

Casanovas-Vilar I, Luján ÀH (2022) Description of the type specimen of the extinct Tenerife giant rat (*Canariomys bravoi*). J Mamm Evol 29(3):645–661. https://doi.org/10.1007/s10914-021-09594-1

Clegg SM, Owens PF, (2002) The 'island rule' in birds: medium body size and its ecological explanation. Proc R Soc Lond B 269(1498):1359–1365. https://doi.org/10.1098/rspb.2002.2024

Crowley B, Yanes Y, Mosher S, Rando J (2019) Revisiting the foraging ecology and extinction history of two endemic vertebrates from tenerife, Canary Islands. Quaternary 2:10. https://doi.org/10.3390/quat2010010

Crusafont-Pairo, M. & Petter, F. (1964). Un muriné géant fossile des îles Canaries *Canariomys bravoi* gen. nov., sp. nov. (rongeurs, muridés). Mammalia 28(4):607–612 https://doi.org/10.1515/mamm.1964.28.4.607

Csiki-Sava Z, Vremir M, Meng J, Brusatte SL, Norell MA (2018) Dome-headed, small-brained island mammal from the Late Cretaceous of Romania. Proc Natl Acad Sci U S A 115(19):4857–4862. https://doi.org/10.1073/pnas.1801143115

Del Arco Aguilar MJ, Rodríguez Delgado O (2018). Vegetation of the Canary Islands. Springer, Cham. https://doi.org/10.1007/978-3-319-77255-4

Delany MJ, Monro RH (1986) Population dynamics of *Arvicanthis niloticus* (Rodentia: Muridae) in Kenya. J Zool 209(1): 85–103. https://doi.org/10.1111/j.1469-7998.1986.tb03567.x

Dobigny G, Tatard C, Gauthier P, Ba K, Duplantier JM, Granjon L, Kergoat GJ (2013) Mitochondrial and nuclear genes-based phylogeography of *Arvicanthis niloticus* (Murinae) and sub-Saharan open habitats Pleistocene history. PLoS One 8(11): e77815. https://doi.org/10.1371/journal.pone.0077815

Dozo MT, Paulina-Carabajal A, Macrini TE, Walsh S (2023) Paleoneurology of Amniotes: New Directions in the Study of Fossil Endocasts. Springer, Cham

Edinger T (1964) Midbrain exposure and overlap in mammals. Am Zool 4(1):5–19. https://doi.org/10.1093/icb/4.1.5

Fadda C, Corti M (2001) Three-dimensional geometric morphometrics of *Arvicanthis*: implications for systematics and taxonomy. J Zool Syst Evol 39(4):235–245. https://doi.org/10.1046/j.1439-0469.2001.00169.x

Fernández Villoldo JA, Verzi DH, Lopes RT, Dos Reis SF, Pérez SI (2023) Brain size and shape diversification in a highly diverse South American clade of rodents (Echimyidae): a geometric morphometric and comparative phylogenetic approach. Biol J Linn Soc 140(2):277–295. https://doi.org/10.1093/biolinnean/blad071

Fernández-Palacios JM, De Nascimento L, Otto R, Delgado JD, García-del-Rey E, Arévalo JR, Whittaker RJ (2011) A reconstruction of Palaeo-Macaronesia, with particular reference to the long-term biogeography of the Atlantic Island laurel forests: Palaeo-Macaronesia and the Atlantic Island laurel forests. J Biogeogr 38(2):226–246. https://doi.org/10.1111/j.1365-2699.2010.02427.x

Firmat C, Rodrigues HG, Renaud S, Claude J, Hutterer R, Garcia-Talavera F, Michaux J (2010) Mandible morphology, dental microwear, and diet of the extinct giant rats *Canariomys* (Rodentia: Murinae) of the Canary Islands (Spain): the extinct Canarian giant rats. Biol J Linn Soc 101(1):28–40. https://doi.org/10.1111/j.1095-8312.2010.01488.x

Flink T, Werdelin L (2022) Digital endocasts from two late Eocene carnivores shed light on the evolution of the brain at the origin of Carnivora. Pap Palaeontol 8(2):e1422. https://doi.org/10.1002/spp2.1422

Gibbard PL, Head MJ (2020) The Quaternary Period. In Gradstein FM, Ogg JG, Schmitz MD, Ogg GM (eds) Geologic Time Scale 2020. Elsevier, Amsterdam, pp 1217–1255. https://doi.org/10.1016/B978-0-12-824360-2.00030-9

Goedert J, Cochard D, Lenoble A, Lorvelec O, Pisanu B, Royer A (2020) Seasonal demography of different black rat (*Rattus rattus*) populations under contrasting natural habitats in Guadeloupe (Lesser Antilles, Caribbean). Mamm Res 65(4):793–804. https://doi.org/10.1007/s13364-020-00523-w

Goyens J, Baeckens S, Smith ESJ, Pozzi J, Mason MJ (2022) Parallel evolution of semicircular canal form and sensitivity in subterranean mammals. J Comp Physiol 208(5–6):627–640. https://doi.org/10.1007/s00359-022-01578-7

Harrington AR, Silcox MT, Yapuncich GS, Boyer DM, Bloch JI (2016). First virtual endocasts of adapiform primates. J Hum Evol 99:52–78. https://doi.org/10.1016/j.jhevol.2016.06.005

Herczeg G, Gonda A, Merilä J, (2009) Evolution of gigantism in nine-spined sticklebacks. Evolution 63(12):3190–3200. https://doi.org/10.1111/j.1558-5646.2009.00781.x

Hutterer R, Lopez-Martinez N, Michaux J (1988) A new rodent from Quaternary deposits of the Canary Islands and its relationships with Neogene and Recent murids of Europe and Africa. Palaeovertebrata 18:241–262.

Itescu Y, Karraker NE, Raia P, Pritchard PCH, Meiri S (2014) Is the island rule general? Turtles disagree. Glob Ecol Biogeogr 23(6):689–700. https://doi.org/10.1111/geb.12149

Jerison HJ (2012) Evolution of The Brain and Intelligence. Elsevier, Amsterdam. https://doi.org/10.1016/B978-0-123-85250-2.X5001-9

Kassambara A, Mundt F (2020) Factoextra: Extract and Visualize the Results of Multivariate Data Analyses, R package v. 1.0. 7. https://doi.org/10.32614/CRAN.package.factoextra

Köhler M, Moyà-Solà S (2004) Reduction of brain and sense organs in the fossil insular bovid *Myotragus*. Brain Behav Evol 63(3):125–140. https://doi.org/10.1159/000076239

Korpimäki E (1985) Prey choice strategies of the Kestrel *Falco tinnunculus* in relation to available small mammals and other Finnish birds of prey. Ann Zool Fenn 22:91–104.

Lang MM, Bertrand OC, San Martin-Flores G, Law CJ, Abdul-Sater J, Spakowski S, Silcox MT (2022) Scaling patterns of cerebellar petrosal lobules in Euarchontoglires: Impacts of ecology and

phylogeny. Anat Rec 305(12):3472–3503. https://doi.org/10.1002/ar.24929
Lê S, Josse J, Husson F (2008) FactoMineR: an R package for multivariate analysis. J Stat Softw 25(1):1–18. https://doi.org/10.18637/jss.v025.i01
Lecompte E, Aplin K, Denys C, Catzeflis F, Chades M, Chevret P (2008) Phylogeny and biogeography of African Murinae based on mitochondrial and nuclear gene sequences, with a new tribal classification of the subfamily. BMC Evol Biol 8(1):199. https://doi.org/10.1186/1471-2148-8-199
Lesson RP (1842) Nouveau Tableau du Règne Animal: Mammifères. Wentworth Press, London.
Liakopoulou D, Roussiakis S, Lyras G (2024) The brain of *Myotragus balearicus*, an insular bovid from the Balearics. Hist Biol 37(8):1880–1887. https://doi.org/10.1080/08912963.2024.2406962
Lomolino MV (1985) Body size of mammals on islands: The island rule reexamined. Am Nat 125(2):310–316.
Lomolino MV (2005) Body size evolution in insular vertebrates: generality of the island rule. J Biogeogr 32(10):1683–1699. https://doi.org/10.1111/j.1365-2699.2005.01314.x
Lomolino MV, Sax DF, Palombo MR, Van Der Geer A (2012) Of mice and mammoths: evaluations of causal explanations for body size evolution in insular mammals. J Biogeogr 39(5): 842–854. https://doi.org/10.1111/j.1365-2699.2011.02656.x
Lomolino MV, Van Der Geer A, Lyras G, Palombo MR, Sax DF, Rozzi R (2013) Of mice and mammoths: generality and antiquity of the island rule. J Biogeogr 40(8): 1427–1439. https://doi.org/10.1111/jbi.12096
Long A, Bloch JI, Silcox MT (2015) Quantification of neocortical ratios in stem primates. Am J Phys Anthropol 157(3):363–373. https://doi.org/10.1002/ajpa.22724
López-Jurado LF, López Martínez N (1987) Un nuevo múrido gigante del cuaternario de Gran Canaria: *Canariomys tamarani* nov. sp. (Rodentia, Mammalia): interpretación filogenética y biogeográfica. Doñana Publ Occas 2:7–60.
López-Torres S, Bertrand OC, Lang MM, Silcox MT, Fostowicz-frelik Ł, Meng J (2023) Cranial endocast of *Anagale gobiensis* (Anagalidae) and its implications for early brain evolution in Euarchontoglires. Palaeontology 66(3):e12650. https://doi.org/10.1111/pala.12650
Lösel PD, van de Kamp T, Jayme A, Ershov A, Faragó T, Pichler O, Tan Jerome N, Aadepu N, Bremer S, Chilingaryan SA, Heethoff M, Kopmann A, Odar J, Schmelzle S, Zuber M, Wittbrodt J, Baumbach T, Heuveline V (2020) Introducing Biomedisa as an open-source online platform for biomedical image segmentation. Nat Commun 11(1):5577. https://doi.org/10.1038/s41467-020-19303-w
Lyras GA (2018) Brain changes during phyletic dwarfing in elephants and hippos. Brain Behav Evol 92(3–4):167–181. https://doi.org/10.1159/000497268
Macrini TE, Rougier GW, Rowe T (2007) Description of a cranial endocast from the fossil mammal *Vincelestes neuquenianus* (Theriiformes) and its relevance to the evolution of endocranial characters in therians. Anat Rec 290(7):875–892. https://doi.org/10.1002/ar.20551
Martínez Méndez F (1966) El extinto múrido gigante *Canariomys bravoi* Crus. et Pet, sus características anatómicas y su evolución. Dissertation, University of Barcelona.
McFadden K W, Meiri S (2013) Dwarfism in insular carnivores: a case study of the pygmy raccoon. J Zool 289(3):213–221. https://doi.org/10.1111/j.1469-7998.2012.00978.x
Meiri S, Cooper N, Purvis A (2008) The island rule: made to be broken? Proc R Soc B 275(1631):141–148. https://doi.org/10.1098/rspb.2007.1056
Meng J, Hu Y, Li C, (2003) The osteology of *Rhombomylus* (Mammalia, Glires): implications for phylogeny and evolution of Glires. Bull Am Mus Nat Hist 275:1–247. https://doi.org/10.1206/0003-0090(2003)275%3C0001:TOORMG%3E2.0.CO;2
Michaux J, López-Martínez N, Hernández-Pacheco JL (1996) The dating of *Canariomys bravoi*, the extinct giant rat from Tenerife (Canary Islands) and the recent history of the endemic species in the archipelago. Vie Milieu 46:261–266.
Michaux J, Hautier L, Hutterer R, Lebrun R, Guy F, García-Talavera F (2012) Body shape and life style of the extinct rodent *Canariomys bravoi* (Mammalia, Murinae) from Tenerife, Canary Islands (Spain). C R Palevol 11(7):485–494. https://doi.org/10.1016/j.crpv.2012.06.004
Monadjem A, Taylor PJ, Denys C, Cotterill FPD (2015) Rodents of Sub-Saharan Africa. A biogeographic and taxonomic synthesis. Walter de Gruyter, Berlin. https://doi.org/10.1515/9783110301915
Moncunill-Solé B, Jordana X, Marín-Moratalla N, Moyà-Solà S, Köhler M (2014) How large are the extinct giant insular rodents? New body mass estimations from teeth and bones. Integr Zool 9(2):197–212. https://doi.org/10.1111/1749-4877.12063
Montesinos R, Da Silva HR, De Carvalho ALG (2012) The 'Island Rule' Acting on Anuran Populations (Bufonidae: *Rhinella ornata*) of the Southern Hemisphere. Biotropica 44(4):506–511. https://doi.org/10.1111/j.1744-7429.2011.00835.x
Oliver WLR, Cox CR, Gonzales PC, Heaney LR (1993) Cloud rats in the Philippines — preliminary report on distribution and status. Oryx 27(1):41–48. https://doi.org/10.1017/S0030605300023942
Orgebin p, Van Der Geer A, Lyras G, Mennecart B, Métais G, Rozzi R (2025) Virtual endocast of the Late Miocene *Hoplitomeryx matthei* (Artiodactyla, Hoplitomerycidae) and brain evolution in insular ruminants. R Soc B Biol Sci 292(2054): 20251542. https://doi.org/10.1098/rspb.2025.1542
Orliac MJ, Gilissen E (2012) Virtual endocranial cast of earliest Eocene *Diacodexis* (Artiodactyla, Mammalia) and morphological diversity of early artiodactyl brains. Proc R Soc B: Biol Sci 279(1743):3670–3677. https://doi.org/10.1098/rspb.2012.1156
Orliac MJ, Argot C, Gilissen E (2012) Digital cranial endocast of *Hyopsodus* (Mammalia, "Condylarthra"): a case of Paleogene terrestrial echolocation? PLoS One 7(2):e30000. https://doi.org/10.1371/journal.pone.0030000
Orliac MJ, Maugoust J, Balcarcel A, Gilissen E (2023) Paleoneurology of Artiodactyla, an overview of the evolution of the artiodactyl brain. In: Dozo MT, Paulina-Carabajal A, Macrini TE, Walsh S (eds) Paleoneurology of Amniotes: New Directions in the Study of Fossil Endocasts. Springer International Publishing, Cham, pp 507–555.
Palmer M (2002) Testing the "island rule" for a tenebrionid beetle (Coleoptera, Tenebrionidae). Acta Oecol 23:103–107. https://doi.org/10.1016/S1146-609X(02)01140-2
Palombo MR, Köhler M, Moyà-Solà S, Giovinazzo C (2008) Brain versus body mass in endemic ruminant artiodactyls: A case studied of *Myotragus balearicus* and smallest *Candiacervus* species from Mediterranean Islands. Quat Int 182(1):160–183. https://doi.org/10.1016/j.quaint.2007.08.037
Perrin MR (1982) Prey specificity of the barn owl, *Tyto alba*, in the Great Fish River valley of the Eastern Cape Province. S Afr J Wildl Res 12(1):14–25. https://doi.org/10.10520/AJA03794369_3454
Pilleri G, Gihr M, Kraus C (1984) Cephalization in rodents with particular reference to the Canadian beaver (Castor canadensis). In: Pilleri G (ed) Investigations on Beavers. Brain Anatomy Institute, Berne, pp 11–102
Quintana J, Köhler M, Moyà-Solà S (2011) *Nuralagus rex*, gen. et sp. nov., an endemic insular giant rabbit from the Neogene of

Minorca (Balearic Islands, Spain). J Vertebr Paleontol 31(2):231–240. https://doi.org/10.1080/02724634.2011.550367
R Core Team (2019) R: a language and environment for statistical computing. R Foundation for Statistical Computing. https://www.Rproject.org/
Rabiu S, Fisher M (1989) The breeding season and diet of *Arvicanthis* in northern Nigeria. J Trop Ecol 5(4):375–386. https://doi.org/10.1017/S0266467400003837
Rando JC, Alcover JA, Galván B, Navarro JF (2014) Reappraisal of the extinction of *Canariomys bravoi*, the giant rat from Tenerife (Canary Islands). Quat Sci Rev 94:22–27. https://doi.org/10.1016/j.quascirev.2014.04.013
Renom P, De-Dios T, Civit S, Llovera L, Sánchez-Gracia A, Lizano E, Rando JC, Marquès-Bonet T, Kergoat GJ, Casanovas-Vilar I, Lalueza-Fox C (2021) Genetic data from the extinct giant rat from Tenerife (Canary Islands) points to a recent divergence from mainland relatives. Biol Lett 17(12):20210533. https://doi.org/10.1098/rsbl.2021.0533
Rowe TB, Macrini TE, Luo ZX (2011) Fossil evidence on origin of the mammalian brain. Science 332(6032):955–957. https://doi.org/10.1126/science.1203117
Sánchez Marco A (2010) New data and an overview of the past avifaunas from the Canary Islands. Ardeola 57(1):13–40.
Schuck-Paim C, Alonso WJ, Ottoni EB, (2008) Cognition in an ever-changing world: climatic variability is associated with brain size in neotropical parrots. Brain Behav Evol 71(3):200–215. https://doi.org/10.1159/000119710
Selås V (1993) Selection of avian prey by breeding Sparrowhawks *Accipiter nisus* in southern Norway: The importance of size and foraging behaviour of prey. Ornis Fenn 70(3):144–154.
Selås V, Tveiten R, Aanonsen OM (2007) Diet of Common Buzzards *Buteo buteo* in southern Norway determined from prey remains and video recordings. Ornis Fenn 84(3):97–104.
Silcox MT, Benham AE, Bloch JI (2010). Endocasts of *Microsyops* (Microsyopidae, Primates) and the evolution of the brain in primitive primates. J Hum Evol 58(6):505 521 https://doi.org/10.1016/j.jhevol.2010.03.008
Sol D (2009) Revisiting the cognitive buffer hypothesis for the evolution of large brains. Biol Lett 5(1):130–133. https://doi.org/10.1098/rsbl.2008.0621
Sol D, Bacher S, Reader SM, Lefebvre L (2008) Brain size predicts the success of mammal species introduced into novel environments. Am Nat 172(1):63–71. https://doi.org/10.1086/588304
Sondaar PY (1977) Insularity and its effect on mammal evolution. In: Hecht MK, Goody PC Hecht BM (eds) Major Patterns in Vertebrate Evolution. Springer, New York, pp 671–707. https://doi.org/10.1007/978-1-4684-8851-7_23
Steppan SJ, Schenk JJ (2017) Muroid rodent phylogenetics: 900-species tree reveals increasing diversification rates. PLoS One 12(8):e0183070. https://doi.org/10.1371/journal.pone.0183070
Suchodoletz HV, Blanchard H, Hilgers A, Radtke U, Fuchs M, Dietze M, Zöller L, (2012). TL and ESR dating of Middle Pleistocene lava flows on Lanzarote Island, Canary Islands (Spain). Quat Geochronol 9:54–64. https://doi.org/10.1016/j.quageo.2012.01.002
Taylor KD, Green MG (1976) The influence of rainfall on diet and reproduction in four African rodent species. J Zool 180(3): 367–389. https://doi.org/10.1111/j.1469-7998.1976.tb04683.x
Van Der Geer A (2014) Parallel patterns and trends in functional structures in extinct island mammals. Integr Zool 9(2):167–182. https://doi.org/10.1111/1749-4877.12066
Van Der Geer A, Lomolino MV, Lyras G (2018) On being the right size – Do aliens follow the rules? J Biogeogr *45*(3):515–529. https://doi.org/10.1111/jbi.13159
Van Der Geer A, Lyras G, De Vos J (2021) Evolution of Island Mammals: Adaptation and Extinction of Placental Mammals on Islands. John Wiley & Sons, New Jersey.
Van Valen L (1973) Body size and numbers of plants and animals. Evol 27(1):27–35. https://doi.org/10.2307/2407116
Vincent F, Souron A, Bertrand OC (2023). The impact of seasonality on the relative brain size of mammals: A test study using extant black rat (*Rattus rattus*) populations from the Lesser Antilles. Eur Assoc Vertebr Palaeontolog Conf Abstr 1:267. https://doi.org/10.18563/pv.eavp2023
Wahlert JH (1974) The cranial foramina of protrogomorphous rodents: An anatomical and phylogenetic Study. Bull Mus Comp Zool 146:363–410.
Walter H (1979) Vegetation of the Earth and Ecological Systems of the Geo-biosphere. Springer, New York. https://doi.org/10.1007/978-1-4684-0468-5
Wible JR (1990) Petrosals of Late Cretaceous marsupials from North America, and a cladistic analysis of the petrosal in therian mammals. J Vertebr Paleontol 10(2):183–205. https://doi.org/10.1080/02724634.1990.10011807
Wible JR (2022) Petrosal and cranial vascular system of the early Eocene palaeoryctid *Eoryctes melanus* from northwestern Wyoming, USA. Acta Palaeontol Pol 67(1):203–220. https://doi.org/10.4202/app.00916.2021
Wible JR, Shelley SL (2020) Anatomy of the petrosal and middle ear of the brown rat, *Rattus norvegicus* (Berkenhout, 1769) (Rodentia, Muridae). Ann Carnegie Mus 86(1):1. https://doi.org/10.2992/007.086.0101
Wickham H (2009) Ggplot2. Springer New York. https://doi.org/10.1007/978-0-387-98141-3
Wilson IDE, Lacher TE, Mittermeier RA (2017) Handbook of the Mammals of the World. Vol. 6. Lagomorphs and Rodents II. Lynx Edicions, Barcelona.
Xiong B, Li A, Lou Y, Chen S, Long B, Peng J, Yang Z, Xu T, Yang X, Li X, Jiang T, Luo Q, Gong H (2017) Precise cerebral vascular atlas in stereotaxic coordinates of whole mouse brain. Front Neuroanat 11:128. https://doi.org/10.3389/fnana.2017.00128